[American Journal of Science, Vol. 322, December, 2022, P. 1124–1158, DOI 10.2475/10.2022.02]

TECHNICAL REPORT

THE PATCH LAB V1.0: A DATABASE AND WORKSPACE FOR CENOZOIC TERRESTRIAL PALEOCLIMATE AND ENVIRONMENT RECONSTRUCTION

TYLER KUKLA*,**,†, JEREMY K. C. RUGENSTEIN**, ELIZABETH DRISCOLL**, DANIEL E. IBARRA***,§, and C. PAGE CHAMBERLAIN*

ABSTRACT. In the last two decades, analytical advances and a growing interest in relevant research questions has brought a rapid increase in the amount of stable isotope data used for reconstructing terrestrial paleoclimates and environments. As the spatial and temporal resolution of proxy data continues to improve, the quantitative interpretation of these data is becoming increasingly common. These advances in data resolution and theory bring opportunities for multi-proxy comparisons, synthesis and modeling of large datasets, integration with paleoecological datasets, improved climate model benchmarking, and more. Here, in an effort to support these growing avenues of research, we present *The PATCH Lab* (Paleo-Analysis of Terrestrial Climate and Hydrology)—an online portal to discover, download, and quantitatively analyze deep time (>1 Ma) terrestrial stable isotope data. The PATCH Lab portal hosts a new database that currently includes 27009 stable isotope measurements from 211 publications spanning multiple terrestrial proxies, and quantitative models for interpreting water isotope and soil carbonate data. Data query, download, and modeling results are organized into user-friendly graphical interfaces that export datasets as .csv files. New data can be easily submitted to the PATCH Lab curators through the portal by completing a data submission template. The PATCH Lab, with the help of community engagement, serves as a resource for archiving terrestrial stable isotope data, building paleo "isoscapes", and increasing accessibility to quantitative methods of investigating terrestrial stable isotopes in paleoclimate.

Key words: Stable isotope, database, Cenozoic, terrestrial, oxygen, hydrogen, carbon

INTRODUCTION

Stable isotopes of oxygen, hydrogen, and carbon from terrestrial "proxy" materials are valuable tracers of water and climate on land throughout Earth history. In this paper, we will refer to these proxy data collectively as "terrestrial stable isotope data," although we recognize these terms cast a broader net. We refrain from a survey of isotope systematics, proxy archives, and interpretation here, but we refer the interested reader to a suite of excellent review papers that help build this foundation (Talbot 1990; Gat 1996; Cerling 1999; Kohn and Cerling 2002; Rowley and Garzione 2007; Sachse and others, 2012; Tabor and Myers 2015; Sharp 2017; Zamanian and others, 2016; Caves Rugenstein and Chamberlain 2018; Bowen and others, 2019; Passey and Levin 2021). The terrestrial stable isotope systems mentioned above are used to address a wide array of problems spanning the growth and death of mountain ranges (Criss and Taylor 1983; Horton and others, 2004; Mulch and others, 2006; Saylor and others, 2009; Hough and others, 2014; Cassel and others, 2018; Bershaw and others, 2019; Methner and others, 2021), patterns of past atmospheric circulation (Quade

* Department of Geological Sciences, Stanford University, Stanford, California, USA
** Department of Geosciences, Colorado State University, Fort Collins, Colorado, USA
*** Institute at Brown for Environment and Society, Brown University, Providence, Rhode Island, USA
§ Department of Earth, Environmental, and Planetary Science, Brown University, Providence, Rhode Island, USA
† Corresponding author: Tyler.Kukla@colostate.edu

and others, 1989; Amundson and others, 1996; Zhisheng and others, 2005; Passey and others, 2009; Suarez and others, 2011; Winnick and others, 2013; Caves and others, 2015), changes in vegetation (Quade and others, 1989; Quade and Cerling 1995; Latorre and others, 1997; Fox and Koch 2003; Zhisheng and others, 2005; Passey and others, 2009; Mix and others, 2013; Caves and others, 2016), atmospheric pCO_2 (Cerling 1999; Ekart and others, 1999; Breecker 2013; Breecker and Retallack 2014; Ji and others, 2018; Da and others, 2019), surface temperatures (Zanazzi and others, 2007; Hough and others, 2014; Mix and Chamberlain 2014; Fan and others, 2018), and more. As such, terrestrial stable isotope tracers are some of the most widely used tools for reconstructing the history of climate, landscapes, and life.

Decades of research have generated a wealth of terrestrial stable isotope data, achieving impressive resolution over space and time and across numerous proxy systems. The publications generating these data represent immeasurable hours of field and laboratory work, and they help form the foundation of our current understanding of deep time (here, >1 Ma) terrestrial climate, tectonics, and environments (Rowley and Garzione 2007; Strömberg 2011; Chamberlain and others, 2012). With advances in laboratory precision and higher throughput methods, new work is rapidly building on this foundation. The high pace of data output brings exciting opportunities for terrestrial stable isotope research, as well as the growing challenge of keeping up with new results. In order to preserve the existing knowledge base and ensure old and new data remain equally accessible into the future, dataset syntheses are a useful next step.

Synthesizing these stable isotope data in a curated database carries additional benefits beyond improving data accessibility. Specifically, a database helps investigators identify and target key gaps in existing records for future studies. Having a central data repository also makes it easier to determine which data gaps are likely to provide the latest information per sampling effort. Much like pieces of a puzzle, the amount of new information that any measurement can provide is limited, but it increases when there are complementary data nearby for comparison to further constrain the plausible interpretations. Research progresses faster when it is easier to find the gaps that likely contribute most to a given research question.

Databases also amplify the role of proxy data in climate model experiments by providing a source for model benchmarking or initialization (Botsyun and Ehlers 2021; Belem and others, 2022). Advances in the spatial and temporal resolution of data have been mirrored by theoretical advances with process-based models designed for paleo-reconstruction (Cerling 1999; Hendricks and others, 2000; Evans and others, 2013; Winnick and others, 2014; Dee and others, 2015a; Dee and others, 2015b; Ibarra and Chamberlain 2015; Caves and others, 2016; Bailey and others, 2018; Dee and others, 2018; Kukla and others, 2019). These models simulate isotopic systems while limiting the number of assumptions and free parameters, bridging the gap between empirical data and complex General Circulation Models (GCMs) or Earth System Models (ESMs). As data coverage improves, so does the utility and potential application of these models. Lastly, databases make existing data accessible to a far wider community than has traditionally utilized such data. Given the increasing ease with which stable isotopes are measured, an increasing number of Earth science subdisciplines are utilizing these measurements to constrain their research questions. By making existing data available, we increase the accessibility to related subdisciplines to utilize the full panoply of constraints that terrestrial stable isotope data have provided in understanding Earth's past.

Here, we present *The PATCH Lab v1.0* (Paleo-Analysis of Terrestrial Climate and Hydrology)—an online platform that merges a multi-proxy terrestrial stable isotope database with quantitative models for analyzing data. Our platform is inspired by ongoing efforts in compiling large, paleo datasets such as in the SISAL database (Atsawawaranunt and others, 2018; Comas-Bru and others, 2020), Macrostrat (Peters and others, 2018), Neotoma (Williams and others, 2018), Iso2k (Konecky and others, 2020), and other compilations (Fox and others, 2018; Kaufman and others, 2020; Jolivet and Boulvais 2021), filling a gap in pre-Quaternary terrestrial proxy data availability. The PATCH Lab includes a portal to find and download the stable isotope data, graphical user interfaces (GUIs) for oxygen (Hendricks and others, 2000; Chamberlain and others, 2014; Winnick and others, 2014; Kukla and others, 2019) and carbon (Cerling 1999; Caves and others, 2016) isotope models, and templates and instructions for submitting new data, data corrections, comments, and queries. The main goals of the database and workspace are twofold: (*1*) to make the spatial dimension (that is, "isoscapes") more accessible for deep time terrestrial studies, and (*2*) to increase the accessibility of quantitative tools for paleoclimate data analysis.

DATABASE OVERVIEW

The first release of the database currently focuses on Cenozoic-age (~66 Ma–present) sediment in North America, Europe, and Asia (fig. 1). Ongoing work is focused on compiling data from additional continents and time periods. Much of the youngest, Quaternary data are not included in the PATCH Lab because these have been compiled in other places such as the SISAL database for cave records (Atsawawaranunt and others, 2018; Comas-Bru and others, 2020). While some older and younger intervals are underrepresented in the database, we welcome new data from these or other points in geologic time. Broadly, any terrestrial stable isotope proxy dataset including oxygen, hydrogen, carbon, clumped, and triple-oxygen isotopes is eligible to be submitted to the database.

Data in version 1.0 were compiled from 211 publications with a total of 27009 measurements including oxygen ($\delta^{18}O$), carbon ($\delta^{13}C$), and hydrogen (δD) isotopes, as well as triple-oxygen ($\Delta^{17}O$) and carbonate clumped measurements (Δ_{47}) when available (table 1). Of these, 24906 are $\delta^{18}O$ measurements, 22114 are $\delta^{13}C$, and 978 are δD. About 59% of the non-biogenic data comes from paleosol strata, 27% from lacustrine sediments, 2% from ashes, and 1% from altered igneous or metamorphic rock. About 23% of the data comes from biogenic material such as shells and tooth enamel.

Proxy Coverage Case Study: Western North America

While it is challenging to quantify the completeness of the existing data record, in North America we have the unique opportunity to compare the density of stable isotope sampling to the estimated distribution of terrestrial sediment via the *Macrostrat* database (Peters and others, 2018). This exercise does not inform the global coverage of stable isotope data, but it does illustrate the regional density of sample coverage and how it has increased through time (fig. 2).

The *Macrostrat* database includes geographic polygons that are fixed through time and represent interpolated lithological boundaries (Peters and others, 2018). Thus, the spatial coverage of a given column is not likely to accurately represent the spatial coverage of the lithology. Instead, we can consider the areal coverage of polygons as a proxy for the upper bound on the true lithological extent. Using these polygons, we extract just the terrestrial sediment lithologies through the Cenozoic to approximate the maximum potential proxy coverage for a given point in time. We note that not all stable isotope proxies are restricted to terrestrial sediments—altered igneous and metamorphic rocks have been used to infer past meteoric water isotopes, for example—but sedimentary proxies make up the vast majority of data in our database (>98%).

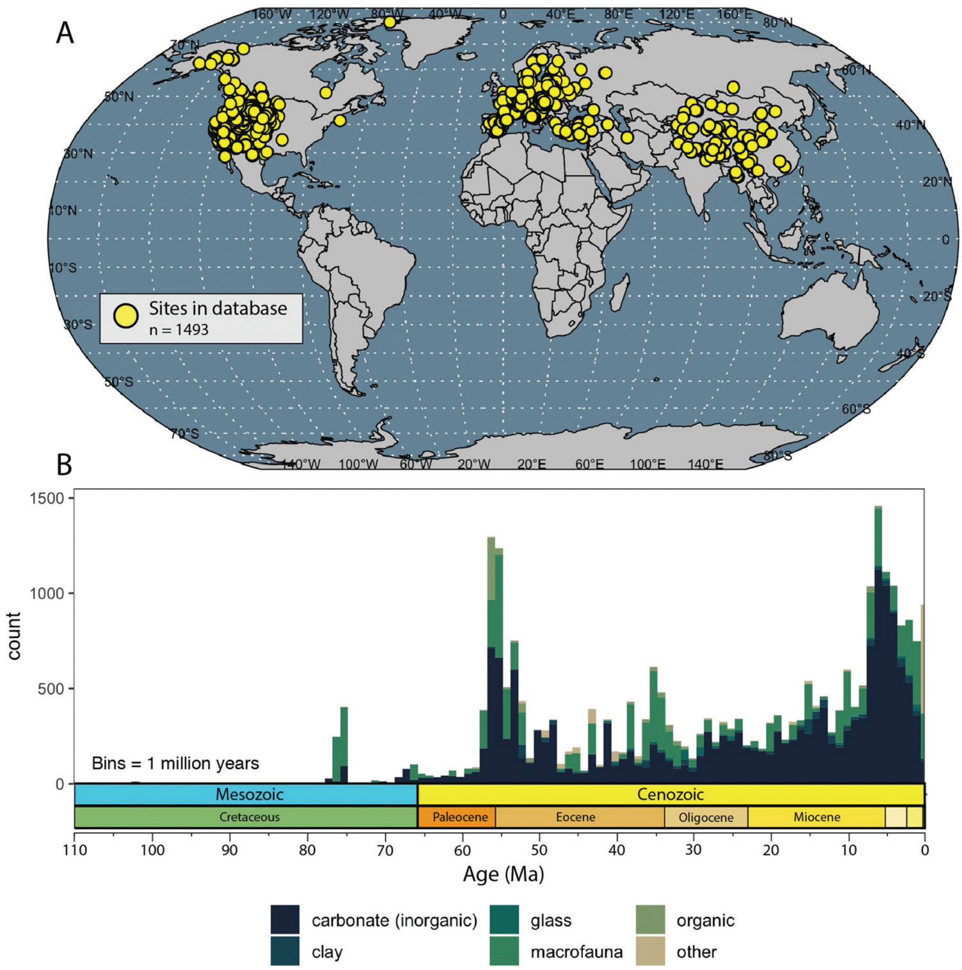

Fig. 1. (A) Global map of proxy data sites represented in the database as of February 2022. (B) Histogram of the number of isotope samples by sample type through time. Note peaks during climate events like the Paleocene-Eocene Thermal Maximum (PETM) and Eocene-Oligocene boundaries. Bins are one million years.

When analyzing Cenozoic sediments, more than half of the terrestrial sediment polygons in western North America have been sampled for stable isotope proxy data (fig. 2b). Together, these polygons account for up to 75% of the total areal coverage of terrestrial sediment in the mid-to-late Cenozoic (fig. 2a). Most of the sampling of individual polygons occurred by 2010, but the few additional polygons sampled from 2010 to present account for a large fraction of the total areal coverage. This result is somewhat sensitive to the time binning used, with the percent of polygons and area sampled increasing with bin duration. We bin the data in 5 million year intervals because this is similar to or greater than the age uncertainty for many terrestrial sections, and consistent with the timescales considered for the tectonic evolution of mountain ranges (Chamberlain and others, 2012). The extensive sample coverage of western North America demonstrates that climate and tectonics reconstructions on a regional (>100 km) scale have grown increasingly tractable as data coverage approaches the coverage of the sedimentary record.

Table 1

Papers included in the database. The data entries column refers to the number of unique sample IDs

	Reference	Sample type(s)	Data entries
1	(Abels and others, 2012)	inorganic carbonate (paleosol + fluvial)	288
2	(Abruzzese, and others, 2005)	other, inorganic carbonate lacustrine	96
3	(Alçiçek and Jiménez-Moreno 2013)	inorganic carbonate (paleosol + fluvial), inorganic carbonate lacustrine	38
4	(Alonso-Zarza and Arenas 2004)	inorganic carbonate (paleosol + fluvial)	29
5	(Amundson and others, 1996)	inorganic carbonate (paleosol + fluvial)	51
6	(Anadón and others, 2015)	shell	101
7	(Andrews, Riding, and Dennis 1997)	other, inorganic carbonate (paleosol + fluvial), shell, inorganic carbonate lacustrine	78
8	(Arehart and O'Neil 1993)	high temperature	16
9	(Arenas and others, 1997)	inorganic carbonate lacustrine	137
10	(Arppe and Karhu 2010)	mammal	120
11	(Baczynski and others, 2013)	inorganic carbonate (paleosol + fluvial), organic	330
12	(Bajnóczi and others, 2006)	inorganic carbonate (paleosol + fluvial)	32
13	(Ballato and others, 2010)	inorganic carbonate (paleosol + fluvial), inorganic carbonate lacustrine	181
14	(Bataille and others, 2016)	inorganic carbonate (paleosol + fluvial)	341
15	(Bentaleb and others, 2006)	mammal	20
16	(Bershaw and others, 2012)	inorganic carbonate (paleosol + fluvial)	13
17	(Bershaw and others, 2019)	volcanic glass	13
18	(Bill and others, 2018)	phyllosilicate	57
19	(Boardman and Secord 2013)	mammal	114
20	(Bougeois and others, 2018)	inorganic carbonate (paleosol + fluvial), other, inorganic carbonate lacustrine	91
21	(Bowen and Bowen 2008)	inorganic carbonate (paleosol + fluvial)	47
22	(Bowen and others, 2001)	inorganic carbonate (paleosol + fluvial)	354
23	(Bowen and others, 2005)	inorganic carbonate (paleosol + fluvial)	145
24	(Bowen and others, 2015)	inorganic carbonate (paleosol + fluvial)	290
25	(Burgener and others, 2019)	inorganic carbonate (paleosol + fluvial)	53
26	(Campani and others, 2012)	inorganic carbonate (paleosol + fluvial), phyllosilicate	209
27	(Carroll and others, 2008)	inorganic carbonate lacustrine	136
28	(Cassel and others, 2009)	volcanic glass	32
29	(Cassel and others, 2012)	volcanic glass	18
30	(Cassel and others, 2014)	volcanic glass	22
31	(Cassel and others, 2018)	volcanic glass	85
32	(Caves and others, 2014)	inorganic carbonate (paleosol + fluvial)	122
33	(Caves and others, 2016)	inorganic carbonate (paleosol + fluvial), inorganic carbonate lacustrine	94
34	(Caves and others, 2017)	inorganic carbonate (paleosol + fluvial)	82
35	(Chamberlain and others, 2012)	inorganic carbonate (paleosol + fluvial), inorganic carbonate lacustrine, phyllosilicate	674
36	(Chamberlain and others, 2020)	high temperature	45

Table 1

(continued)

	Reference	Sample type(s)	Data entries
37	(Charreau and others, 2012)	inorganic carbonate (paleosol + fluvial)	216
38	(Clyde and others, 2010)	inorganic carbonate (paleosol + fluvial)	78
39	(Criss and Taylor 1983)	high temperature	1
40	(Crowley and others, 2008)	mammal	147
41	(Csonka and others, 2020)	inorganic carbonate (paleosol + fluvial)	43
42	(Currie and others, 2005)	inorganic carbonate (paleosol + fluvial)	7
43	(Currie and others, 2016)	inorganic carbonate (paleosol + fluvial)	12
44	(Cyr and others, 2005)	inorganic carbonate lacustrine	39
45	(Davis and others, 2008)	inorganic carbonate lacustrine	205
46	(Davis, Mix, and others, 2009a)	inorganic carbonate lacustrine	184
47	(Davis, Mulch, and others, 2009b)	inorganic carbonate lacustrine	209
48	(Dean and others, 2015)	inorganic carbonate lacustrine	1524
49	(DeCelles and others, 2007)	inorganic carbonate (paleosol + fluvial)	31
50	(DeCelles and others, 2011)	inorganic carbonate (paleosol + fluvial)	15
51	(Dettman and Lohmann 2000)	shell	618
52	(Dettman and others, 2001)	shell, mammal	401
53	(Dettman and others, 2003)	inorganic carbonate (paleosol + fluvial), inorganic carbonate lacustrine	141
54	(Ding and Yang 2000)	inorganic carbonate (paleosol + fluvial)	220
55	(Ding and others, 2014)	inorganic carbonate lacustrine, inorganic carbonate (paleosol + fluvial)	56
56	(Doebbert and others, 2010)	inorganic carbonate lacustrine	212
57	(Domingo and others, 2013)	mammal	298
58	(Dong and others, 2018)	inorganic carbonate (paleosol + fluvial)	384
59	(Eren 2011)	inorganic carbonate (paleosol + fluvial)	24
60	(Fan and Dettman 2009)	shell	981
61	(Fan and others, 2011)	inorganic carbonate (paleosol + fluvial)	32
62	(Fan and others, 2014a)	inorganic carbonate lacustrine, inorganic carbonate (paleosol + fluvial), shell	25
63	(Fan and others, 2014b)	volcanic glass	72
64	(Fan and others, 2017)	inorganic carbonate (paleosol + fluvial), shell	204
65	(Fan and others, 2018)	inorganic carbonate (paleosol + fluvial)	108
66	(Fan and others, 2021)	shell, inorganic carbonate (paleosol + fluvial)	426
67	(Foreman and others, 2011)	shell, inorganic carbonate (paleosol + fluvial), inorganic carbonate lacustrine, fish	9
68	(Foreman and others, 2015)	inorganic carbonate (paleosol + fluvial), shell	94
69	(Fox and Koch 2003)	inorganic carbonate (paleosol + fluvial)	274
70	(Fox and Koch 2004)	inorganic carbonate (paleosol + fluvial)	28
71	(Fox and others, 2012)	inorganic carbonate (paleosol + fluvial)	194
72	(Fricke and Wing 2004)	fish, mammal	39
73	(Fricke and others, 1998)	mammal, fish	210

TABLE 1

(continued)

	Reference	Sample type(s)	Data entries
74	(Fricke and others, 2008)	fish, reptile, shell, inorganic carbonate (paleosol + fluvial)	157
75	(Fricke and others, 2010)	inorganic carbonate (paleosol + fluvial), shell	68
76	(Fricke 2003)	mammal	47
77	(Gallant and others, 2014)	inorganic carbonate (paleosol + fluvial)	26
78	(Garzione and others, 2000)	inorganic carbonate (paleosol + fluvial)	34
79	(Gébelin and others, 2012)	inorganic carbonate lacustrine, high temperature	68
80	(Genty and others, 2003)	other	300
81	(Ghosh and others, 2004)	inorganic carbonate (paleosol + fluvial)	64
82	(Godfrey and others, 2018)	inorganic carbonate (paleosol + fluvial)	167
83	(Harris and others, 2020)	mammal	227
84	(Harzhauser and others, 2007)	shell	117
85	(Harzhauser and others, 2012)	shell	164
86	(Heitmann and others, 2017)	inorganic carbonate (paleosol + fluvial)	145
87	(Hellwig and others, 2018)	inorganic carbonate (paleosol + fluvial)	78
88	(Hofman-Kamińska and others, 2018)	mammal	116
89	(Hoke and others, 2014)	inorganic carbonate (paleosol + fluvial)	118
90	(Honegger and others, 2020)	inorganic carbonate (paleosol + fluvial)	149
91	(Horton and Chamberlain 2006)	inorganic carbonate lacustrine, phyllosilicate	213
92	(Horton and others, 2004)	inorganic carbonate lacustrine, other, phyllosilicate	134
93	(Hough and others, 2011)	inorganic carbonate (paleosol + fluvial), inorganic carbonate lacustrine	218
94	(Hren and others, 2010)	organic	20
95	(Huntington and others, 2009)	inorganic carbonate lacustrine	7
96	(Huntington and others, 2010)	inorganic carbonate lacustrine	70
97	(Huntington and others, 2011)	shell, inorganic carbonate (paleosol + fluvial)	11
98	(Huyghe and others, 2017)	other	28
99	(Hyland and Sheldon 2013)	inorganic carbonate (paleosol + fluvial), organic	58
100	(Hyland and others, 2013)	inorganic carbonate (paleosol + fluvial), organic	32
101	(Ibarra and others, 2021)	other, inorganic carbonate lacustrine	23
102	(Ingalls and others, 2018)	inorganic carbonate (paleosol + fluvial), inorganic carbonate lacustrine	72
103	(Jensen and others, 2020)	mammal	41
104	(Jiang and others, 2002)	inorganic carbonate (paleosol + fluvial)	73
105	(Kaakinen and others, 2006)	inorganic carbonate (paleosol + fluvial)	96
106	(Kelson and others, 2018)	inorganic carbonate (paleosol + fluvial)	35
107	(Kent-Corson and others, 2006)	inorganic carbonate (paleosol + fluvial)	183
108	(Kent-Corson and others, 2009)	inorganic carbonate (paleosol + fluvial), inorganic carbonate lacustrine, other	1383
109	(Kent-Corson and others, 2010)	inorganic carbonate (paleosol + fluvial)	91

Table 1

(continued)

	Reference	Sample type(s)	Data entries
110	(Kent-Corson and others, 2013)	inorganic carbonate (paleosol + fluvial), inorganic carbonate lacustrine	134
111	(Kluge and Affek 2012)	other	27
112	(Koch and others, 1995)	inorganic carbonate (paleosol + fluvial), mammal	217
113	(Koch and others, 2003)	inorganic carbonate (paleosol + fluvial), organic	460
114	(Kocsis and others, 2014)	mammal	219
115	(Kohn and Law 2006)	mammal, fish	337
116	(Kohn and others, 2002)	mammal	207
117	(Kovács and others, 2012)	mammal	36
118	(Kovács and others, 2015)	mammal	57
119	(Kovda and others, 2008)	inorganic carbonate (paleosol + fluvial)	44
120	(Küçükuysal and Kapur 2014)	inorganic carbonate (paleosol + fluvial)	11
121	(Kukla and others, 2021b)	phyllosilicate	84
122	(Lacroix and Niemi 2019)	inorganic carbonate lacustrine	32
123	(Latorre and others, 1997)	mammal	46
124	(Leary and others, 2017)	inorganic carbonate (paleosol + fluvial)	43
125	(Lechler and Niemi 2011)	inorganic carbonate lacustrine	4
126	(Leone and others, 2000)	inorganic carbonate (paleosol + fluvial), shell	126
127	(Li and others, 2015)	inorganic carbonate lacustrine, shell	50
128	(Li and others, 2016a)	inorganic carbonate (paleosol + fluvial)	288
129	(Li and others, 2016b)	inorganic carbonate (paleosol + fluvial), inorganic carbonate lacustrine	128
130	(Li and others, 2021)	volcanic glass	60
131	(Licht and others, 2014)	mammal, shell	268
132	(Licht and others, 2017b)	inorganic carbonate (paleosol + fluvial)	66
133	(Licht and others, 2017a)	inorganic carbonate (paleosol + fluvial), inorganic carbonate lacustrine, other	46
134	(Licht and others, 2020)	inorganic carbonate (paleosol + fluvial), organic	438
135	(Liu and others, 2014)	inorganic carbonate (paleosol + fluvial), inorganic carbonate lacustrine	
136	(Lüdecke and others, 2013)	inorganic carbonate lacustrine	230
137	(Lukens and others, 2017)	inorganic carbonate (paleosol + fluvial), other	69
138	(Macaulay and others, 2016)	inorganic carbonate (paleosol + fluvial)	35
139	(Mack and Cole 2005)	inorganic carbonate (paleosol + fluvial)	5
140	(Mack and others, 1994)	inorganic carbonate (paleosol + fluvial)	31
141	(Matson and Fox 2010)	mammal	181
142	(Matson and others, 2012)	organic, inorganic carbonate (paleosol + fluvial)	66
143	(McFadden and others, 2015)	high temperature	10
144	(McLean and Bershaw 2021)	inorganic carbonate (paleosol + fluvial)	17
145	(Meijers and others, 2016)	inorganic carbonate lacustrine	162
146	(Meijers and others, 2018)	inorganic carbonate lacustrine	101

Table 1

(continued)

	Reference	Sample type(s)	Data entries
147	(Methner and others, 2015)	high temperature, other	85
148	(Methner and others, 2016b)	inorganic carbonate (paleosol + fluvial)	123
149	(Methner and others, 2016a)	inorganic carbonate (paleosol + fluvial), inorganic carbonate lacustrine	161
150	(Methner and others, 2020)	inorganic carbonate (paleosol + fluvial)	114
151	(Mix and Chamberlain 2014)	phyllosilicate	231
152	(Mix and others, 2013)	inorganic carbonate (paleosol + fluvial)	55
153	(Mix and others, 2016)	phyllosilicate	34
154	(Mix and others, 2019)	inorganic carbonate (paleosol + fluvial), inorganic carbonate lacustrine, phyllosilicate	165
155	(Mulch and others, 2006)	phyllosilicate	34
156	(Mulch and others, 2007)	high temperature, other	39
157	(Mulch and others, 2008)	volcanic glass	83
158	(Mulch and others, 2015)	inorganic carbonate (paleosol + fluvial), inorganic carbonate lacustrine, phyllosilicate	72
159	(Mullin, ms, 2010)	inorganic carbonate (paleosol + fluvial)	31
160	(Nehme and others, 2020)	other	4
161	(Ortiz and others, 2006)	shell	424
162	(Page and others, 2019)	inorganic carbonate (paleosol + fluvial)	20
163	(Passey and others, 2009)	inorganic carbonate (paleosol + fluvial), mammal	293
164	(Peryam and others, 2011)	inorganic carbonate (paleosol + fluvial)	47
165	(Poage and Chamberlain 2002)	inorganic carbonate (paleosol + fluvial), phyllosilicate, inorganic carbonate lacustrine	40
166	(Poulson and John 2003)	inorganic carbonate lacustrine	27
167	(Quade and others, 1989)	inorganic carbonate (paleosol + fluvial)	111
168	(Quade and others, 1994)	inorganic carbonate (paleosol + fluvial), organic, mammal	60
169	(Quade and others, 1995)	inorganic carbonate (paleosol + fluvial)	48
170	(Retallack and others, 2004)	inorganic carbonate (paleosol + fluvial)	355
171	(Ring and others, 2020)	mammal	41
172	(Rothe and others, 1974)	shell, other	76
173	(Rowe and others, 2020)	other	421
174	(Rowley and Currie 2006)	inorganic carbonate lacustrine, inorganic carbonate (paleosol + fluvial)	3
175	(San Jose and others, 2020)	inorganic carbonate (paleosol + fluvial), other, inorganic carbonate lacustrine, shell	274
176	(Sanyal and others, 2005)	inorganic carbonate (paleosol + fluvial)	64
177	(Saylor and others, 2009)	inorganic carbonate lacustrine	252
178	(Scherler,2014)	mammal	92
179	(Schlunegger and others, 2007)	inorganic carbonate (paleosol + fluvial)	54
180	(Schwartz and others, 2019)	inorganic carbonate lacustrine, inorganic carbonate (paleosol + fluvial)	74

TABLE 1
(continued)

	Reference	Sample type(s)	Data entries
181	(Sjostrom and others, 2006)	phyllosilicate	62
182	(Smith and others, 1993)	inorganic carbonate (paleosol + fluvial)	52
183	(Smith and others, 2017)	volcanic glass	14
184	(Spencer and others, 1996)	shell	2
185	(Stern and others, 1997)	phyllosilicate, inorganic carbonate (paleosol + fluvial)	68
186	(Sun and others, 2017)	inorganic carbonate (paleosol + fluvial), inorganic carbonate lacustrine	176
187	(Super, ms, 2010)	phyllosilicate	18
188	(Takeuchi and Larson 2005)	phyllosilicate	17
189	(Takeuchi and others, 2010)	inorganic carbonate (paleosol + fluvial)	117
190	(Takeuchi 2007)	phyllosilicate	55
191	(Tang and others, 2017)	inorganic carbonate (paleosol + fluvial)	28
192	(Ting and others, 2003)	inorganic carbonate (paleosol + fluvial)	59
193	(Torres and Gaines 2013)	inorganic carbonate (paleosol + fluvial)	25
194	(Tütken and others, 2008)	mammal	49
195	(Vasilyan and Carnevale 2013)	inorganic carbonate (paleosol + fluvial)	24
196	(Vögeli and others, 2017)	inorganic carbonate (paleosol + fluvial)	48
197	(Wang and Deng 2005)	mammal	126
198	(Wang and others, 1993)	inorganic carbonate (paleosol + fluvial), inorganic carbonate lacustrine, mammal	59
199	(Wang and others, 1996)	inorganic carbonate (paleosol + fluvial)	3
200	(Wei and others, 2016)	inorganic carbonate lacustrine	58
201	(White and Schiebout 2008)	inorganic carbonate (paleosol + fluvial)	123
202	(White and others, 2001)	inorganic carbonate (paleosol + fluvial)	11
203	(White and others, 2017)	phyllosilicate	9
204	(Winnick and others, 2013)	inorganic carbonate (paleosol + fluvial)	106
205	(Xu and others, 2013)	inorganic carbonate (paleosol + fluvial), inorganic carbonate lacustrine	35
206	(Xu and others, 2015)	inorganic carbonate (paleosol + fluvial)	37
207	(Xu and others, 2016)	inorganic carbonate (paleosol + fluvial), inorganic carbonate lacustrine	11
208	(Zamarreno and others, 1997)	inorganic carbonate (paleosol + fluvial), inorganic carbonate lacustrine	111
209	(Zanazzi and others, 2007)	mammal	548
210	(Zanazzi and others, 2015)	mammal	19
211	(Zhuang and others, 2011)	inorganic carbonate (paleosol + fluvial), inorganic carbonate lacustrine	107

Lacking sufficient *Macrostrat* coverage to repeat this analysis elsewhere, the western North America sample coverage emphasizes the utility of a terrestrial stable isotope database for the Cenozoic. With this expansive, multi-proxy coverage, studies that interpret spatial gradients in isotope ratios (Mulch and others, 2006; Sjostrom and others, 2006; Chamberlain and others, 2012; Fan and others, 2014b; Cassel and others, 2018), differences in isotope ratios between proxies (Stern and others, 1997; Poage and Chamberlain 2002; Tabor and others, 2002; Tabor and Montañez 2005),

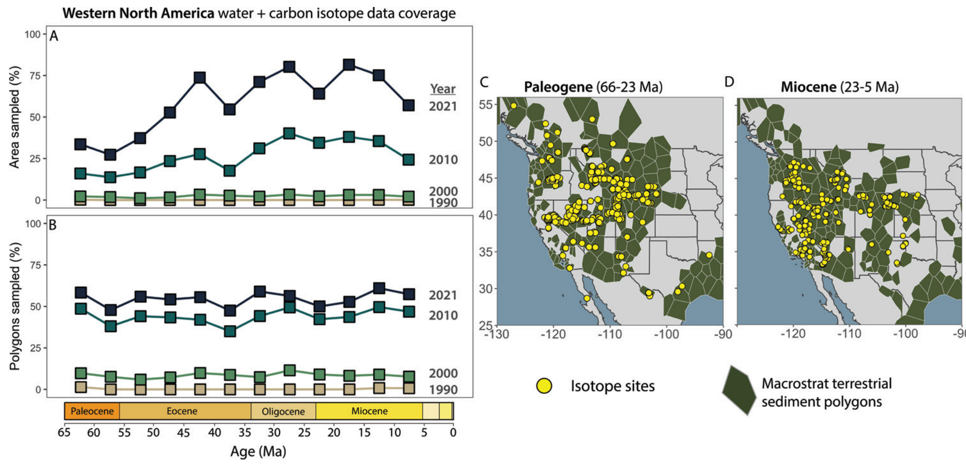

Fig. 2. Estimated coverage of western North America stable oxygen, hydrogen, and carbon isotope data based on comparison with terrestrial sediment in the Macrostrat database. (A) The areal coverage of polygons containing stable isotope data. (B) The fraction of polygons containing stable isotope data. Lines refer to cumulative data coverage as of a given year (ranging from 1990, beige, to 2021, dark blue) (C, D) Maps of present-day dataset locations (yellow circles) overlain on Macrostrat polygons for the Paleogene (C) and Miocene (D).

or other dimensions beyond the outcrop scale are becoming easier and more common. We anticipate that the database presented here will further contribute to this ongoing work to understand data spatially and across proxies.

DATA STRUCTURE

Balancing Data Grouping and Data Integrity

One challenge in synthesizing data is making data easy to extract based on a wide range of dimensions without grouping the data so broadly that useful information is lost. For example, it is not particularly helpful to group all paleosol data by paleosol depth horizon because the depth horizon is not commonly reported. However, it is important to keep the depth horizon information available for those that find it useful for modeling or other purposes (Caves and others, 2016; Gao and others, 2021). To address this problem, we constrain the inputs for each data entry column to one of three input categories—free, flexible, or fixed inputs. These three input types are designed for efficient data queries (with flexible and fixed inputs) and minimal data loss or compromise relative to the original publication (with free inputs).

Free input columns are those that accept any values (numeric, character, date, *etc*) usually related to notes or descriptions about the data, locality, sample, or sedimentary interpretation. For example, a free input column might note the specific name of a sample site, how the age model was constructed, or the accuracy of the listed coordinates. Due to the flexibility of free input columns, they are not very useful for querying data but are useful for contextualizing and understanding data once it is selected.

Flexible input columns require a specific type of input (like a numeric or character) but the value of the input is not constrained. We use two types of flexible input columns—alphanumeric and numeric flexible inputs. Alphanumeric flexible inputs are publication references or codes that identify entities like a locality or sample. These inputs are flexible, rather than free, because they contain input restrictions such as following a reference format or disallowing spaces or certain characters.

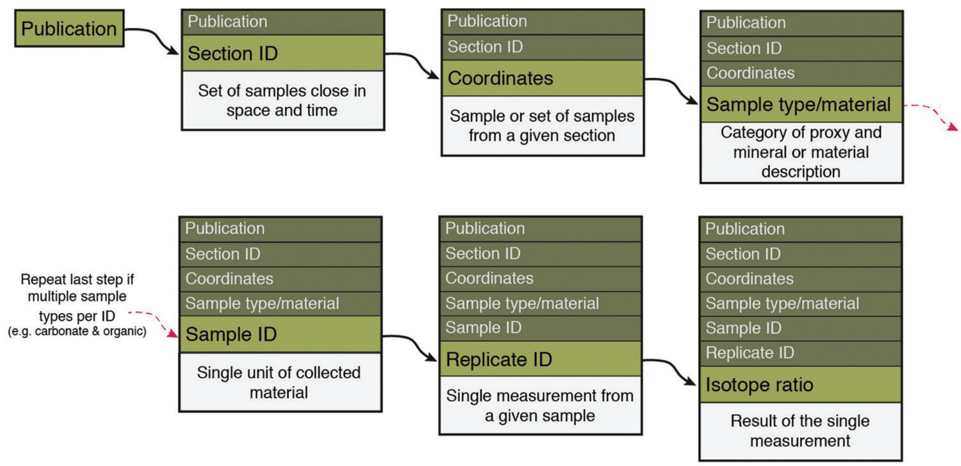

Fig. 3. Illustrated data hierarchy for flexible queries. Red arrow marks duplicating Sample IDs assigned by the original author if the same sample is run for more than one isotope proxy system.

Numeric flexible inputs (restricted to numbers) include columns such as the age of the sample or its isotopic ratio. Numeric flexible input columns are useful for querying data based on quantitative characteristics such as geographic range (latitude and longitude) or age range (for example, the Eocene, 56–34 Ma).

Fixed inputs columns allow only a fixed set of input values. Fixed input columns are used for broad grouping of data types by defining the sample material and its basic lithology or fossil source. They also include columns that accept binary values (yes or no) that are useful for data filtering (for example, to remove duplicated values that were published in one paper and compiled in a later paper). Fixed input columns are designed for querying qualitative data characteristics, such as data from a specific mineral or type of deposit (for example, paleosol versus lacustrine carbonate). Together, these three column input types are designed to meet a range of data query and post-processing goals while minimizing the amount of information that is lost or condensed.

Data Fields Hierarchy

Any given stable isotope value rests on a hierarchy of information designed to simplify data querying and post-processing steps (fig. 3). The basic unit of this structure is the publication (or a dataset ID in cases where data comes from publicly available MS and PhD theses). While a more basic unit would be a given sample basin or locality, we use the publication because not all samples are linked to a given basin (for example, altered igneous or metamorphic rock) and the publication unit simplifies the data entry step, especially in cases where the sampling basin is not reported and must be independently determined.

Within every publication, we define at least one section ID. Section IDs are flexible alphanumeric inputs that separate groups of samples by space and geologic time. Often, they are defined based on how the original publication grouped data. When no groupings are available, we define a single section ID as a group of data from a continuous or near-continuous sedimentary package, sampled within an areal range of tens of kilometers or less. This definition is not rigid (that is, there is no strict geographic or temporal cut-off between section IDs) because we want to account for cases where nearby sections in space and time show distinct results. For example, if two outcrops of the same age a few kilometers apart have distinct isotope ratios, we will preserve this distinction by assigning separate section IDs, despite their close spatial and temporal proximity. Therefore, users that wish to group data by section ID do not lose this information.

After the section ID, the next delineations are the sample coordinates, sample grouping, and sample ID. Coordinates (latitude [−90,90] and longitude [−180,180)) are flexible numeric inputs reported in decimal degrees (positive in the north and east directions) to the resolution of the original paper unless otherwise noted. In cases where the coordinates are not reported, we make an estimate based on the available information (often a map figure or survey systems such as the section, township and range survey location previously used in the United States) and note our approximation. The sample type and sample material are flexible alphanumeric inputs. There are two sample type columns recording similar information in more general and specific terms. The basic sample type defines a given sample based on its lithological, mineralogical, or fossil origin (for example, "phyllosilicate" or "shell") and the more specific sample type distinguishes between sub-categories (for example, "altered ash" or "mollusc"). The sample material denotes the mineral or material measured (for example, "smectite" or "aragonite"). Finally, the sample ID is a flexible alphanumeric identification code assigned by the original paper or, when none is available, generated by us. We deviate from the sample ID defined by the original paper if multiple sample types are measured for a given sample ID. In this case, we append a suffix to the sample ID that distinguishes the sample type (such as "XXorg" and "XXcarb" for organic and carbonate carbon measurements of the same hand sample).

The last two delineations, the replicate ID (flexible alphanumeric) and isotope ratio (flexible numeric), refer to individual measurements. The replicate ID distinguishes individual measurements of a single sample and is often defined based on the sample ID and some suffix (such as "1, 2, 3 . . ."). In cases where the sample was not replicated, the replicate and sample IDs are identical or replicate IDs are left blank. In some cases, only the average isotope ratio of multiple samples is reported (and individual measurements are not available), and we enter the isotope ratio as if it were a single measurement and note that the value reflects the average of multiple measurements. Finally, the isotope ratio is the last level of the hierarchy, and is a numeric value assigned to one of 5 columns ($\delta^{18}O$, $\delta^{13}C$, δD, Δ_{47}, $\Delta^{17}O$). All data in a given column are reported relative to the same isotope standard (VSMOW for oxygen and hydrogen isotopes, converted from VPDB where necessary, and VPDB for carbon isotopes).

All column names are grouped by their data input type (free, flexible, or fixed) and described in table 2. Aside from the hierarchical inputs outlined in figure 3, other columns provide sample-specific information like the outcrop height and age uncertainty as well as notes about the data or decisions made during data entry. For a full list of the column input restrictions by column, see the database user guide in the Supplementary Information.

Integration with Related Data

In some cases, measurements beyond stable oxygen, hydrogen, and carbon isotopes are published with the isotope data that are useful for data interpretation. For example, strontium isotope data may be useful for constraining drainage sources in lacustrine carbonates. Similarly, if multiple measurements are made from different locations on a sample (such as mammal teeth) it can be useful to know the distance along the sample where the material was taken. In order to include these complementary data, we add six generic data entry columns—three to define data types ("Other_data_type_X") and three to define data values ("Other_data_value_X"). In these columns, the value "X" can be either "1," "2," or "3," and this number links the data type and value. While many

TABLE 2

Name and description of all data entry columns in the database

Data entry category	Column header	Description	Example input
Fixed	Sample_type_basic	General designation of sample type	inorganic carbonate lacustrine
Fixed	Sample_type	Lithologic or fossil origin of sample	Altered ash
Fixed	Sample_material	Mineral or sample material measured	kaolinite
Fixed	Previously_published	Yes (Y) or no (N) denoting if the measurement was also published in an earlier paper (useful for papers that present compilations)	N
Fixed	Event	Name of climate or other event covered by the section or a set of samples	PETM
Fixed	Event_excursion?	Yes (Y) or no (N) denoting if the sample occurs during a transient excursion (for filtering with long-term data)	Y
Fixed	Author_upload	Yes (Y) if data was uploaded by the author or person generating the new data, no (N) if uploaded by PATCH Lab curators.	N
Flexible (alphanumeric)	Reference	Original publication or data entry contact (for unpublished data)	Abels and others, 2012
Flexible (alphanumeric)	Reference_ID	Unique alphanumeric code for the reference	ABELS12
Flexible (alphanumeric)	Section_ID	Unique alphanumeric code for the section site	ABELS12_UDC
Flexible (alphanumeric)	Sample_ID	Unique alphanumeric code for the sample	UDC-1
Flexible (alphanumeric)	Replicate_ID	Unique alphanumeric code for replicated measurement	UDC-1a
Flexible (alphanumeric)	PrevPublished_Ref	Reference for the paper where data was originally published (if Previously_published = Y, otherwise blank)	
Flexible (numeric)	Latitude	Sample latitude in decimal degrees	44.2
Flexible (numeric)	Longitude	Sample longitude in decimal degrees (range -180, 180)	-113.5
Flexible (numeric)	Height_m	Stratigraphic height (or depth, if core) of sample in meters	80
Flexible (numeric)	Age_Ma	Assigned sample age in million years ago (Ma)	55

TABLE 2
(continued)

Data entry category	Column header	Description	Example input
Flexible (numeric)	Top_age_Ma	Youngest age uncertainty bound (stratigraphic top)	54
Flexible (numeric)	Bottom_age_Ma	Oldest age uncertainty bound (stratigraphic bottom)	58
Flexible (numeric)	d18O_smow	Oxygen isotope measurement (permille VSMOW)	20
Flexible (numeric)	d13C_pdb	Carbon isotope measurement (permille VPDB)	-4
Flexible (numeric)	dD_smow	Hydrogen isotope measurement (permille VSMOW)	-120
Flexible (numeric)	D17O_permille	Triple-oxygen isotope measurement	-0.20
Flexible (numeric)	D17O_lambda	Triple-oxygen isotope slope for calculation	0.528
Flexible (numeric)	D47_permille	Clumped isotope measurement	0.500
Flexible (numeric)	d18Oprecip_smow	Reported composition of meteoric water	-10
Flexible (numeric)	dDprecip_smow	Reported composition of meteoric water	-70
Flexible (numeric)	Other_data_value_X	Value of an additional data type relevant to isotope data (3 columns where X=1, 2, or 3)	65
Free	Other_data_type_X	Type of additional data noted in "Other_data_value_X" (3 columns where X=1, 2, or 3)	Percent carbonate
Free	Sample_notes	Most relevant additional information about sample	Carbonate root cast
Free	Notes_1	Relevant notes about sample or section	Upper Deer Creek section
Free	Notes_2	Relevant notes about sample or section	Bighorn Basin
Free	Data_entry_notes	Details about entry to database	Locations approximate using map in Fig. 1
Free	Published_wateriso _interpretation	Interpreted driver of water isotope value (blank if meteoric or primary fluid)	evaporative
Free	Published_carboniso _interpretation	Interpreted driver of carbon isotope value (blank if primary)	Contamination of young carbon

publications include data beyond terrestrial stable isotope data, we generally only include other data in these columns if they are directly relevant for contextualizing the isotope data. However, new data entries do not need to follow this guideline and are welcome to include any additional data in these generic columns.

Data Entry Decisions and Data Upload Notebooks

While we strive to maintain as much of the original information from a given data entry as possible, the data contributor or curator must make some decisions about how the data are entered. These include decisions about what information is included versus omitted in the entry, as well as how to enter information that is unclear or not explicitly defined by the authors. For example, some papers on the Paleocene Eocene Thermal Maximum report data by time relative to the carbon isotope excursion or by stratigraphic height. This practice is useful for the original study but does not provide a clear path forward for correlating these data with data from other sections that are constrained in time. Though these ages can be left blank, the data may not be queried when a user extracts data by time, thus limiting the search result. A similar issue sometimes emerges for sample coordinates. In some papers, sample locations are shown on a map, but coordinates are not reported in the data tables. The latitude and longitude can be left blank, but at the risk of the data being omitted from geographic queries.

In order to make our data entry practices transparent, we document decisions such as these in Word documents or text files referred to as data upload "notebooks". Each data upload (publication or unpublished dataset entry) has its own notebook, and each notebook contains "General notes" and "Next steps". The general notes section includes decisions about data entry such as those discussed above. These decisions are usually also documented in a notes column in the database itself. The next steps section includes updates that can be made to the data entry in the future. These updates might be to ask the corresponding author for clarification in the case of a data entry question, or for additional data if only average values of multiple replicates are reported. In some cases, the next steps include entering "other data" that is available in the manuscript but does not fall into any of the stable isotope data columns. The next steps efforts do not involve changes to the data entry that are critical for the isotope data (in this case, the isotope data are not made available in the database). Data upload notebooks are maintained offline as part of the data entry workflow and are currently available upon request. Future versions of the PATCH Lab will permit automatic downloading of these notebooks with the selected data.

DATA CURATION AND QUALITY CONTROL

Data curation in the v1.0 database is intentionally minimal. We strive to present the data in a form that is as close to the original publication as possible. In doing so, we avoid screening for the "highest fidelity" data because the fidelity of the data is subjective. It makes sense to screen for fidelity if there is only a single environmental signal of interest, such as paleo-temperature (Kaufman and others, 2020). However, stable isotope proxies are often sensitive to multiple environmental signals, and high fidelity data for one application might be low fidelity data for another. For example, data that faithfully record a soil water evaporation trend may be a useful measure of aridity, but a less useful recorder of meteoric $\delta^{18}O$. To avoid curating such widely applicable data for a single purpose, our quality control efforts are limited to objective tests such as whether numerical data are outliers compared to the database and whether there are typos in the sample type, material, or geographic domain. These basic tests do not catch every type of issue with the data, but they leave little room for curator bias, and they allow the user to apply the data to a wide range of problems.

Some screening criteria could be applied to the bulk database without directly limiting its applicability, such as placing bounds on the analytical precision of allowable data or requiring a minimum number of replicate analyses. We avoid placing such restrictions on the data because the cut-offs are arbitrary and should vary for different proxy materials and analytical methods. As a result, these quality control metrics and others, such as whether the field site is accurately characterized, generally require expertise in the specific proxy and field site—expertise that is better fulfilled by the peer review process than by our small team. Thus, we only accept data that are published in peer reviewed journals or theses (MS or PhD) reviewed by an expert committee.

However, issues may arise with a dataset long after the peer review process. One such issue is that new age models may require updates to old publications. If we know an age model is outdated, we will note this issue in the data, but we will not assign a new age model because doing so generally requires experience and expertise with the site in question, as well as decisions about how to quantify age model uncertainty. We will, however, update data that is re-interpreted with a new age model since, in this case, the application of the new age model is unambiguous. In other cases, we rely on experts in the field to submit necessary corrections (see Sect. 6.1). Another issue is that the preferred calibration and data processing steps for clumped isotope-derived temperatures has changed over time (Bernasconi and others, 2018; Anderson and others, 2021; Bernasconi and others, 2021). Updating the data processing and calibration methods for an old dataset can be time-intensive or even impossible if the original, unprocessed data are not reported. We plan to add functionality for supplemental files to address these issues in v1.1 of the database but, presently, we define the calibration used and refer the data users to the original publication.

We recognize that the decision to minimize our own curation comes with a trade-off. While shielding the data from decisions made by curators who may lack expertise for a given site, we place a larger burden on database users to ensure that the data meets their own standards and project needs. In some cases, a user's specific application will require additional filtering or quality control of the data. For example, many samples are interpreted as “evaporatively enriched,” but the evidence for evaporative enrichment varies drastically across publications. A standardized test for evaporative enrichment across the full database would strengthen internal consistency, but it would also amount to reinterpreting many published records. Our goal is to present, rather than interpret, the data in the database. Thus, beyond the test of peer review, any challenges to the interpretations of the original authors must come from the data user.

THE PATCH LAB PORTAL

The PATCH Lab portal (https://geocentroid.shinyapps.io/PATCH-Lab/) is the web platform that hosts the database and graphical user interface (GUI) models for simulating oxygen and carbon isotopes. While the models can be used in any capacity, we anticipate they will be most useful for placing quantitative constraints on possible interpretations, testing hypotheses, and constraining the sensitivity of stable isotope ratios to various forcings. Output from data queries and model simulations can be downloaded in .csv format for offline analysis and plotting. Additional code for database queries can also be downloaded from Github (https://github.com/tykukla/PATCH-Lab) for offline use.

Querying the Isotope Database

Database queries can be completed from the homepage of The PATCH Lab portal (fig. 4). Here, users will find a variety of filtering options. In the left column, all sample

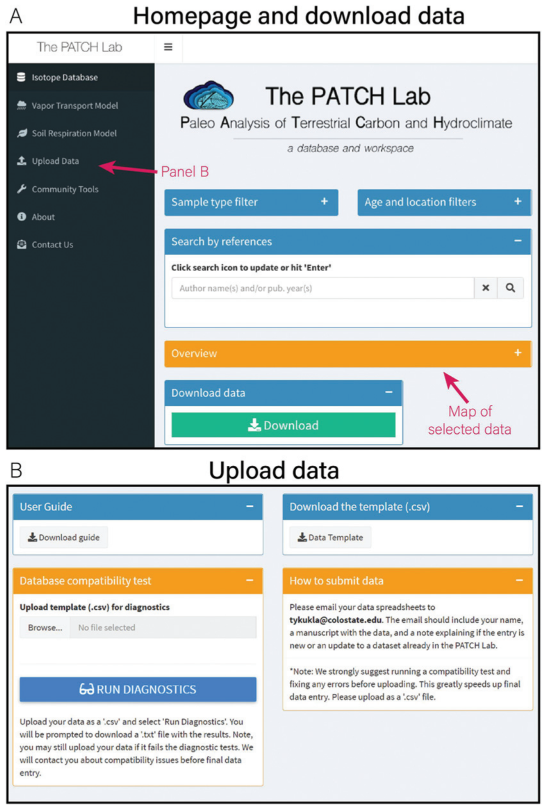

Fig. 4. Portal screenshots for the homepage and data upload page. (A) Homepage panels with a plus (+) icon are collapsed. Bar on left shows all pages on the portal. Overview panel shows a map and histogram as in fig. 1. Green download button returns a .csv file of filtered data. (B) The data upload page has options to download the database user guide and template (blue headers) as well as to test your data spreadsheet for compatibility ("run diagnostics").

types represented in the database are listed and can be selected for a given download. In the right column, samples can be further queried by time, data interpretation ("Filter for meteoric interpretation"), and long-term conditions ("Filter out transient events"). The meteoric interpretation filter removes any sample values that the original authors did not interpret as reflecting primary meteoric water or fluids (for example, samples affected by evaporation, diagenesis, etc.). The transient events filter removes local, transient isotope excursions like the Paleocene Eocene Thermal Maximum. This feature is useful for studies looking at long-term mean conditions, such as for stable isotope paleoaltimetry or for broadly-defined modeling experiments (for example, "Eocene" boundary conditions). Finally, users can select whether to average the output values based on "Measurement number" (averages replicate measurements of a given sample) or "Measurement number & site" (averages replicates and then all samples of a given site). The entire database can be downloaded by selecting all sample types, the full age range, and no filtering or averaging.

Soil Respiration Model Overview

For nearly four decades, carbon isotopes in paleosols have been modeled using a 1-D production-diffusion equation (Cerling, 1984). During that time, a substantial amount of work has refined the soil carbonate paleo-barometer and explored the importance of and controls on the various parameters in the model. For full derivations of the model, we refer the reader to Cerling, 1984; Cerling and others, 1993; Davidson, 1995; Cerling, 1999 and Breecker, 2013. Though the paleosol carbonate paleo-barometer has been most frequently used to estimate past atmospheric pCO_2—particularly for periods when there are few other proxies of pCO_2, such as in the Paleozoic and Mesozoic—recent workers have also inverted the paleo-barometer to quantitatively examine soil respiration rates (Caves and others, 2014, 2016; Caves Rugenstein and Chamberlain, 2018; Licht and others, 2020). Within The PATCH Lab, we include the ability to model both soil respiration rates and atmospheric pCO_2, as well as to forward model and thereby estimate paleosol carbonate $\delta^{13}C$. Using the equations presented in (Cerling, 1999) and (Caves and others, 2016), the built-in soil respiration model includes four different outputs. Output 1 calculates soil respiration at a defined soil column depth given a range of paleosol carbonate $\delta^{13}C$ values as well as other necessary model inputs, such as atmospheric pCO_2 and its isotopic composition, the isotopic composition of respired soil carbon, and the carbonate formation temperature. The output data are $\delta^{13}C$ and soil respiration rate values for a given depth in the soil column. Output 2 solves for the $\delta^{13}C$ as a function of depth in the soil profile using similar inputs as output 1 as well as the soil respiration rate. Output 3 returns atmospheric pCO_2 based on the isotopic composition of soil carbonate and other necessary inputs such as the soil pCO_2 and its isotopic composition. Lastly, output 4 reads in carbon isotope data that is defined in age and uses the compilation of paleo-atmospheric pCO_2 from the Paleo-CO_2 project (https://paleo-co2.org/) to solve for soil respiration rates, propagating the measurement and paleo-pCO_2 uncertainties through. We also remove paleosol-based estimates of past atmospheric pCO_2 to avoid circularity and impose an upper pCO_2 estimate limit of 3000 ppm so the highest values have less effect on both the mean atmospheric pCO_2 used and the estimated mean soil respiration. We note that the paleo-CO_2 database is still under development, and the PATCH Lab data are subject to change as it is updated.

Vapor Transport Model Overview

The vapor transport model simulates oxygen isotopes in vapor, precipitation, and evapotranspiration over space along a 1-dimensional storm track (fig. 5). The water balance and isotope ratios are solved simultaneously as a function of the balance of moisture transport (both advective and eddy diffusive), precipitation, and evapotranspiration fluxes. The model is based on the equations of Hendricks and others, 2000, with modifications for continental applications from Mix and others, 2013; Chamberlain and others, 2014; Winnick and others, 2014; Caves and others, 2015 and Xia and Winnick 2021, and the parameterization of orographic rainout and energetic constraints on evapotranspiration of Kukla and others, 2019.

The model is useful for testing hypotheses for climatic and topographic drivers of $\delta^{18}O$ (Carolin and others, 2019; Kukla and others, 2019; Wolf and others, 2020). Previous applications of the model have also used spatial isotope gradients to reconstruct precipitation rates (Kukla and others, 2021a). The GUI version of the model is necessarily limited but designed to include all of the functionality for flexible single simulations. For the source code of the model, see the supplement of (Kukla and others, 2019) or the Github repository (https://github.com/tykukla/Vapor_Transport_Model_KuklaEtAl2019).

COMMUNITY ENGAGEMENT

Community engagement is critical to The PATCH Lab's goal of bringing robust data and modeling tools to a single, easy-to-access location. There are four main avenues for members of the research community to engage with this effort: (*1*) Data contribution; (*2*) Update requests; (*3*) Code contribution; and (*4*) Long-term project steering.

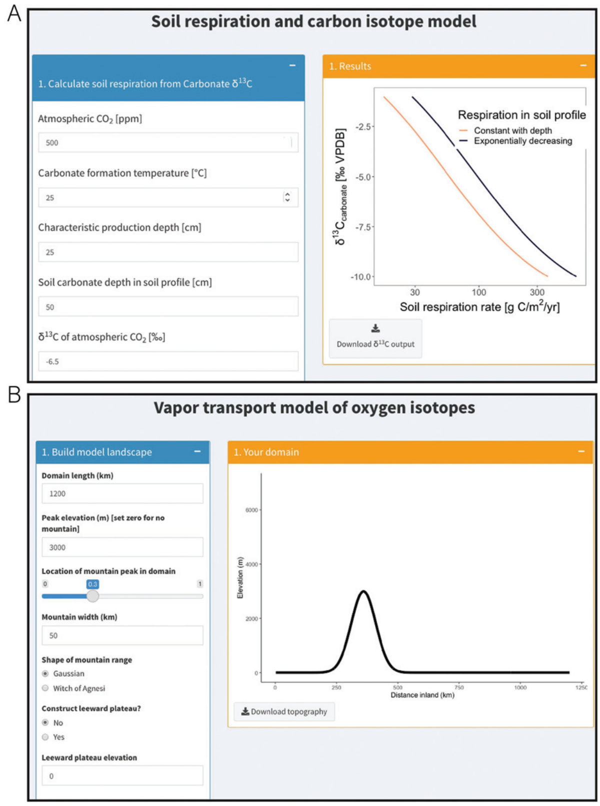

Fig. 5. Graphical User Interface (GUI) example screenshots for the (A) $\delta^{13}C$ and (B) $\delta^{18}O$ models. Left columns (blue headers) are used to initialize the model and the right columns (orange headers) display the output. All model output can be downloaded as a .csv file.

Data Contribution

In addition to data and model downloads, The PATCH Lab portal includes the tools necessary to contribute new data (see fig. 4). A basic workflow for the data contribution process is shown in figure 6. Data contributors can begin by downloading the PATCH Lab template that includes all of the data entry columns listed in table 2 in the correct order. Contributors will also fill out a brief contact sheet so that we can reach out if we have any questions about the data submission.

Once the template is completed, the data contributor can test for compatibility with existing data using the “run diagnostics” button. The diagnostics test compares each column’s data against the restrictions imposed on flexible and fixed input columns, and the result of the test is printed to the screen. Isotope ratios are also compared against the entire database to flag outliers that may reflect a data entry error such as a missing decimal point, negative sign, or incorrect isotope standard. The data contributor can submit the data regardless of the test result; however, we encourage contributors to address errors identified by the test and double-check outlier values or include a note about these errors with the data submission.

The PATCH Lab curators will continue to add data to the database, and we strive to upload recent publications swiftly. We encourage community contributors to upload their own data to minimize the influence of curators on data entry decisions.

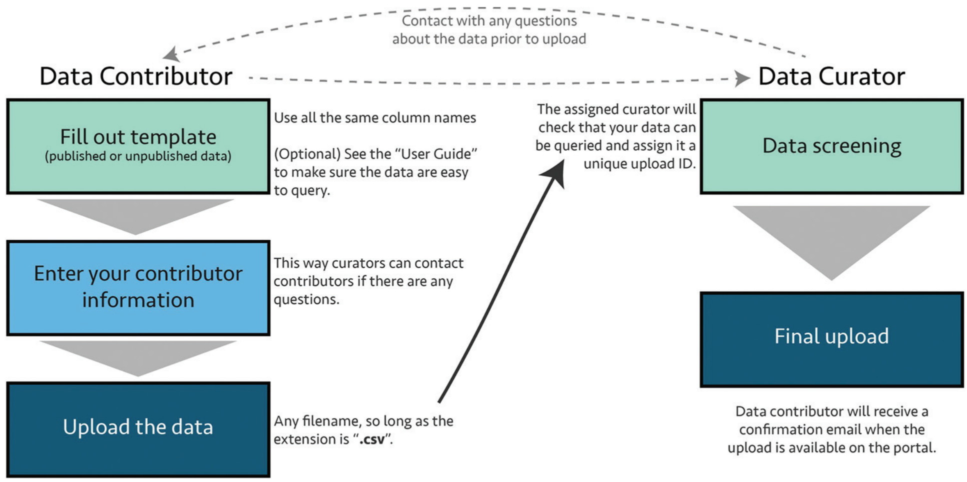

Fig. 6. Flow chart of the data upload process.

Update Requests

Update requests are useful for a range of applications from fixing data entry errors to updating the broader format of the portal. For example, we recognize that the author of a dataset may not agree with decisions made by the data curators during the data entry process. In this case, we encourage the author to contact the curators directly or submit an update request. These requests can range from a message with update instructions to a completed data template to replace the existing entry. Update requests can also be used by data users that notice errors in existing entries. In this case, we will verify the correct data input from the original publication and make the appropriate changes.

We also welcome feedback and requests that are not related to the database. Users that would like to see new functionality, such as changes to model interfaces or the data query process, can contact the curators via The PATCH Lab portal.

Code Contribution

The "Community Tools" page of The PATCH Lab portal hosts links to code developed by the research community that is of interest to other PATCH Lab users. These entries are not restricted to any specific functionality, but some helpful resources include code for processing or plotting data, for running other models, or for integrating other datasets like modern climate, topography, or water isotopes. We also encourage users to contact us about integrating new graphical user interface models into The PATCH Lab portal directly. The portal runs on code written in R, so resources written in R can be easily adapted to be featured on the portal.

Currently, this page includes links to R code to work with the database. There are a variety of scripts, including the same data query scripts used by The PATCH Lab portal, for users to build upon or modify. There are also some functions for statistical analysis that is useful for determining statistical power and possible data biases. We also encourage users to explore statistical tools for working with geologic data and accounting for spatial and temporal uncertainty, such as the monte carlo approaches outlined in Breecker, 2013 and Dzombak and others, 2021. Scripts like these can be sent to PATCH Lab curators to upload to the Community Tools alongside data from a given publication to improve transparency and reproducibility.

Long-Term Steering Committee

The PATCH Lab is advised by a steering committee to help ensure its long-term success and to stay up to date with the needs of different research communities. The steering committee identifies areas of the resource that can be improved and advises on its long-term infrastructure. The committee includes two distinct groups—an advisory panel and regional editors. The primary role of advisory panel members is to identify long-term goals for the PATCH lab and provide feedback from relevant subdisciplines that frequently use terrestrial stable isotope data. In turn, regional editors handle data curation for certain continents or regions and act to identify new data trends that may impact data curation and archiving. Regional editors also identify and upload data that is missing from the database within their region and serve as the point of contact for authors uploading data in their region. Members of the committee are listed in The PATCH Lab portal, and those interested in getting involved are encouraged to reach out via the portal's contact page.

CONCLUDING REMARKS

The PATCH Lab is an online workspace that integrates terrestrial stable isotope data and models for efficient data download and analysis. Previous and ongoing research already leverages the rapid increase in data of the past two decades. However, synthesizing these data on a case-by-case basis will become more challenging and time intensive as the total amount of available data grows. The goal of this effort is to provide a long-term, curated database for research purposes, alongside tools that can assist in data interpretation.

We emphasize that community engagement in this effort is critical to its utility. The PATCH Lab is a tool developed for the terrestrial paleoclimate and environment community—a community that spans a wide range of disciplines and sub-disciplines, each of which may find the tool useful for different reasons. Feedback from, and engagement with, the research community are the most effective ways to ensure this resource remains useful as science progresses.

ACKNOWLEDGMENTS

We thank all of the researchers who generated the stable isotope data compiled in The PATCH Lab. We also thank Nathan Sheldon, Associate Editor Michael Hren, and one anonymous reviewer for comments that significantly improved the manuscript. We are grateful to Hari Mix, Danielle Y. Moragne, and Sam Kramer for their contributions compiling data. We thank Katharina Methner for valuable conversations about the database structure, and Caitlin Mothes and Matthew Ross of the CSU Geospatial Centroid for assistance in hosting the PATCH Lab application. This work was funded by NSF EAR-1322084.

REFERENCES

Abels, H. A., Clyde, W. C., Gingerich, P. D., Hilgen, F. J., Fricke, H. C., Bowen, G. J., and Lourens, L. J., 2012, Terrestrial carbon isotope excursions and biotic change during Palaeogene hyperthermals: Nature Geoscience, v. 5, p. 326–329, https://doi.org/10.1038/ngeo1427

Abruzzese, M. J., Waldbauer, J. R., and Chamberlain, C. P., 2005, Oxygen and hydrogen isotope ratios in freshwater chert as indicators of ancient climate and hydrologic regime: Geochimica et Cosmochimica Acta, v. 69, p. 1377–1390, https://doi.org/10.1016/j.gca.2004.08.036

Alçiçek, H., and Jiménez-Moreno, G., 2013, Late Miocene to Plio-Pleistocene fluvio-lacustrine system in the Karacasu Basin (SW Anatolia, Turkey): Depositional, paleogeographic and paleoclimatic implications: Sedimentary Geology, v. 291, p. 62–83. https://doi.org/10.1016/j.sedgeo.2013.03.014

Alonso-Zarza, A. M., and Arenas, C., 2004, Cenozoic calcretes from the Teruel Graben, Spain: microstructure, stable isotope geochemistry and environmental significance: Sedimentary Geology, v. 167, p. 91–108, https://doi.org/10.1016/j.sedgeo.2004.02.001

Amundson, R., Chadwick, O., Kendall, C., Wang, Y., and DeNiro, M., 1996, Isotopic evidence for shifts in atmospheric circulation patterns during the late Quaternary in mid–North America: Geology, v. 24, n. 1, p. 23–26, https://doi.org/10.1130/0091-7613(1996)024<0023:IEFSIA>2.3.CO;2

Anadón, P., Oms, O., Riera, V., and Julià, R., 2015, The geochemistry of biogenic carbonates as a paleoenvironmental tool for the Lower Pleistocene Barranco León sequence (BL-5D, Baza Basin, Spain): Quaternary international: the journal of the International Union for Quaternary Research, v. 389, p. 70–83, https://doi.org/10.1016/j.quaint.2014.09.062

Anderson, N. T., Kelson, J. R., Kele, S., Daëron, M., Bonifacie, M., Horita, J., Mackey, T. J., John, C. M., Kluge, T., Petschnig, P., Jost, A. B., Huntington, K. W., Bernasconi, S. M., and Bergmann, K. D., 2021, A unified clumped isotope thermometer calibration (0.5–1,100°C) using carbonate-based standardization: Geophysical Research Letters, v. 48, n. 7, p. e2020GL092069, https://doi.org/10.1029/2020GL092069

Andrews, J. E., Riding, R., and Dennis, P. F., 1997, The stable isotope record of environmental and climatic signals in modern terrestrial microbial carbonates from Europe: Palaeogeography, Palaeoclimatology, Palaeoecology, v. 129, p. 171–189, https://doi.org/10.1016/S0031-0182(96)00120-4

Arehart, G. B., and O'Neil, J. R., 1993, D/H ratios of supergene Alunite as an indicator of paleoclimate in continental settings, *in* Swart, P. K., Lohmann, K. C., Mckenzie, J., and Savin, S., editors, Climate Change in Continental Isotopic Records: Washington, D. C., American Geophysical Union, p. 277–284, https://doi.org/10.1029/GM078p0277

Arenas, C., Casanova, J., and Pardo, G., 1997, Stable-isotope characterization of the Miocene lacustrine systems of Los Monegros (Ebro Basin, Spain): palaeogeographic and palaeoclimatic implications. Palaeogeography, Palaeoclimatology, Palaeoecology, 128, n. 1–4, p. 133–155, https://doi.org/10.1016/S0031-0182(96)00052-1

Arppe, L., and Karhu, J. A., 2010, Oxygen isotope values of precipitation and the thermal climate in Europe during the middle to late Weichselian ice age: Quaternary Science Reviews, v. 29, n. 9–10, p. 1263–1275, https://doi.org/10.1016/j.quascirev.2010.02.013

Atsawawaranunt, K., Comas-Bru, L., Amirnezhad Mozhdehi, S., Deininger, M., Harrison, S. P., Baker, A., Boyd, M., Kaushal, N., Ahmad, S. M., Ait Brahim, Y., Arienzo, M., Bajo, P., Braun, K., Burstyn, Y., Chawchai, S., Duan, W., Hatvani, I. G., Hu, J., Kern, Z., Labuhn, I., Lachniet, M., Lechleitner, F. A., Lorrey, A., Pérez-Mejías, C., Pickering, R., and Scroxton, N., 2018, The SISAL database: a global resource to document oxygen and carbon isotope records from speleothems: Earth System Science Data, v. 10, p. 1687–1713, https://doi.org/10.5194/essd-10-1687-2018

Baczynski, A. A., McInerney, F. A., Wing, S. L., Kraus, M. J., Bloch, J. I., Boyer, D. M., Secord, R., Morse, P. E., and Fricke, H. C., 2013, Chemostratigraphic implications of spatial variation in the Paleocene-Eocene Thermal Maximum carbon isotope excursion, SE Bighorn Basin, Wyoming: Bighorn Basin, Wyoming Petm Chemostratigraphy: Geochemistry, Geophysics, Geosystems, v. 14, p. 4133–4152, https://doi.org/10.1002/ggge.20265

Bailey, A., Posmentier, E., and Feng, X., 2018, Patterns of evaporation and precipitation drive global isotopic changes in atmospheric moisture: Geophysical Research Letters, v. 45, n. 14, p. 7093–7101, https://doi.org/10.1029/2018GL078254

Bajnóczi, B., Horváth, Z., Demény, A., and Mindszenty, A., 2006, Stable isotope geochemistry of calcrete nodules and septarian concretions in a Quaternary "red clay" paleovertisol from Hungary: Isotopes in Environmental and Health Studies, v. 42, n. 4, p. 335–350, https://doi.org/10.1080/10256010600991045

Ballato, P., Mulch, A., Landgraf, A., Strecker, M. R., Dalconi, M. C., Friedrich, A., and Tabatabaei, S. H., 2010, Middle to late Miocene Middle Eastern climate from stable oxygen and carbon isotope data, southern Alborz mountains, N Iran: Earth and Planetary Science Letters, v. 300, n. 1–2, p. 125–138, https://doi.org/10.1016/j.epsl.2010.09.043

Bataille, C. P., Watford, D., Ruegg, S., Lowe, A., and Bowen, G. J., 2016, Chemostratigraphic age model for the Tornillo Group: A possible link between fluvial stratigraphy and climate: Palaeogeography, Palaeoclimatology, Palaeoecology, v. 457, p. 277–289, https://doi.org/10.1016/j.palaeo.2016.06.023

Belem, A., Bell, T., Burdett, H. L., Ibarra, D., Kaushal, N., Keenan, B., Klimaszewski-Patterson, A., Mette, M., Naeher, S., Onafeso, O. D., Panmei, C., Ratnayake, A. S., and Truax, O., 2022, Paleoclimatology and paleoceanography perspectives on integrated, coordinated, open, networked (ICON) science: Earth and Space Science, v. 9, n. 1, p. e2021EA002115, https://doi.org/10.1029/2021EA002115

Bentaleb, I., Langlois, C., Martin, C., Iacumin, P., Carré, M., Antoine, P.-O., Duranthon, F., Moussa, I., Jaeger, J.-J., Barrett, N., and Kandorp, R., 2006, Rhinocerotid tooth enamel 18O/16O variability between 23 and 12 Ma in southwestern France: Comptes Rendus: Geoscience, v. 338, n. 3, p. 172–179, https://doi.org/10.1016/j.crte.2005.11.007

Bernasconi, S. M., Müller, I. A., Bergmann, K. D., Breitenbach, S. F. M., Fernandez, A., Hodell, D. A., Jaggi, M., Meckler, A. N., Millan, I., and Ziegler, M., 2018, Reducing uncertainties in carbonate clumped isotope analysis through consistent carbonate-based standardization: Geochemistry, Geophysics, Geosystems, v. 19, n. 9, p. 2895–2914, https://doi.org/10.1029/2017GC007385

Bernasconi, S. M., Daëron, M., Bergmann, K. D., Bonifacie, M., Meckler, A. N., Affek, H. P., Anderson, N., Bajnai, D., Barkan, E., Beverly, E., Blamart, D., Burgener, L., Calmels, D., and Chaduteau, C., and others, 2021, InterCarb: A community effort to improve interlaboratory standardization of the carbonate clumped isotope thermometer using carbonate standards: Geochemistry, Geophysics, Geosystems, v. 22, n. 5 https://doi.org/10.1029/2020GC009588

Bershaw, J., Garzione, C. N., Schoenbohm, L., Gehrels, G., and Tao, L., 2012, Cenozoic evolution of the Pamir plateau based on stratigraphy, zircon provenance, and stable isotopes of foreland basin sediments at Oytag (Wuyitake) in the Tarim Basin (west China): Journal of Asian Earth Sciences, v. 44, p. 136–148, https://doi.org/10.1016/j.jseaes.2011.04.020

Bershaw, J., Cassel, E. J., Carlson, T. B., Streig, A. R., and Streck, M. J., 2019, Volcanic Glass as a Proxy for Cenozoic Elevation and Climate in the Cascade Mountains, Oregon, USA: Journal of Volcanology and Geothermal Research, v. 381, p. 157–67, https://doi.org/10.1016/j.jvolgeores.2019.05.021

Bill, N. S., Mix, H. T., Clark, P. U., Reilly, S. P., Jensen, B. J. L., and Benowitz, J. A., 2018, A stable isotope record of late Cenozoic surface uplift of southern Alaska: Earth and Planetary Science Letters, v. 482, p. 300–311, https://doi.org/10.1016/j.epsl.2017.11.029

Boardman, G. S., and Secord, R., 2013, Stable isotope paleoecology of White River ungulates during the Eocene–Oligocene climate transition in northwestern Nebraska: Palaeogeography, Palaeoclimatology, Palaeoecology, v. 375, p. 38–49, https://doi.org/10.1016/j.palaeo.2013.02.010

Botsyun, S., and Ehlers, T. A., 2021, How can climate models be used in paleoelevation reconstructions? Frontiers in Earth Science, v. 9, p. 624542, https://doi.org/10.3389/feart.2021.624542

Bougeois, L., Dupont-Nivet, G., de Rafélis, M., Tindall, J. C., Proust, J.-N., Reichart, G.-J., de Nooijer, L. J., Guo, Z., and Ormukov, C., 2018, Asian monsoons and aridification response to Paleogene Sea retreat and Neogene westerly shielding indicated by seasonality in Paratethys oysters: Earth and Planetary Science Letters, v. 485, p. 99–110, https://doi.org/10.1016/j.epsl.2017.12.036

Bowen, G. J., and Bowen, B. B., 2008, Mechanisms of PETM Global Change Constrained by a New Record from Central Utah: Geology, v. 36, n. 5, p. 379–382, https://doi.org/10.1130/G24597A.1

Bowen, G. J., Koch, P. L., Gingerich, P. D., Norris, R. D., Bains, S., and Corfield, R. M., 2001, Refined Isotope Stratigraphy Across the Continental Paleocene-Eocene Boundary on Polecat Bench in the Northern Bighorn Basin: Paleocene-Eocene Stratigraphy and Biotic Change in the Bighorn and Clarks Fork Basins, Wyoming, University of Michigan Papers on Paleontology, v. 33, p. 73–88.

Bowen, G. J., Koch, P. L., Meng, J., Ye, J., and Ting, S., 2005, Age and correlation of fossiliferous late Paleocene–early Eocene strata of the erlian basin, inner Mongolia, China: American Museum Novitates, v. 2005, n. 3474, https://doi.org/10.1206/0003-0082(2005)474[0001:AACOFL]2.0.CO;2

Bowen, G. J., Maibauer, B. J., Kraus, M. J., Röhl, U., Westerhold, T., Steimke, A., Gingerich, P. D., Wing, S. L., and Clyde, W. C., 2015, Two massive, rapid releases of carbon during the onset of the Palaeocene–Eocene thermal maximum: Nature Geoscience, v. 8, p. 44–47, https://doi.org/10.1038/ngeo2316

Bowen, G. J., Cai, Z., Fiorella, R. P., and Putman, A. L., 2019, Isotopes in the water cycle: regional- to global-scale patterns and applications: Annual Review of Earth and Planetary Sciences, v. 47 n. 1, p. 453–479, https://doi.org/10.1146/annurev-earth-053018-060220

Breecker, D. O., 2013, Quantifying and understanding the uncertainty of atmospheric CO_2 concentrations determined from calcic paleosols: Geochemistry, Geophysics, Geosystems, v. 14, n. 8, p. 3210–3220, https://doi.org/10.1002/ggge.20189

Breecker, D. O., and Retallack, G. J., 2014, Refining the pedogenic carbonate atmospheric CO_2 proxy and application to Miocene CO_2: Palaeogeography, Palaeoclimatology, Palaeoecology, v. 406, p. 1–8, https://doi.org/10.1016/j.palaeo.2014.04.012

Burgener, L., Hyland, E., Huntington, K. W., Kelson, J. R., and Sewall, J. O., 2019, Revisiting the equable climate problem during the Late Cretaceous greenhouse using paleosol carbonate clumped isotope temperatures from the Campanian of the Western Interior Basin, USA: Palaeogeography, Palaeoclimatology, Palaeoecology, v. 516, p. 244–267, https://doi.org/10.1016/j.palaeo.2018.12.004

Campani, M., Mulch, A., Kempf, O., Schlunegger, F., and Mancktelow, N., 2012, Miocene paleotopography of the central alps: Earth and Planetary Science Letters, v. 337–338, p. 174–185, https://doi.org/10.1016/j.epsl.2012.05.017

Carolin, S. A., Ersek, V., Roberts, W. H. G., Walker, R. T., and Henderson, G. M., 2019, Drying in the middle east during northern hemisphere cold events of the early glacial period: Geophysical Research Letters, v. 46, n. 23, p. 14003–14010, https://doi.org/10.1029/2019GL084365

Carroll, A. R., Doebbert, A. C., Booth, A. L., Chamberlain, C. P., Rhodes-Carson, M. K., Smith, M. E., Johnson, C. M., and Beard, B. L., 2008, Capture of high-altitude precipitation by a low-altitude Eocene lake, western U.S: Geology, v. 36, n. 10, p. 791–794, https://doi.org/10.1130/G24783A.1

Cassel, E. J., Graham, S. A., and Chamberlain, C. P., 2009, Cenozoic Tectonic and Topographic Evolution of the Northern Sierra Nevada, California, Through Stable Isotope Paleoaltimetry in Volcanic Glass: Geology, v. 37, n. 6, p. 547–550, https://doi.org/10.1130/G25572A.1

Cassel, E.J., Graham, S.A., Chamberlain, C.P., and Henry, C.D., 2012, Early Cenozoic Topography, Morphology, and Tectonics of the Northern Sierra Nevada and Western Basin and Range: Geosphere, v. 8, n. 2, p. 229–49, https://doi.org/10.1130/GES00671.1

Cassel, E.J., Breecker, D.O., Henry, C.D., Larson, T.E., and Stockli, D.F., 2014. Profile of a paleo-orogen: High topography across the present-day Basin and Range from 40 to 23 Ma, Geology, v. 42, n. 11, p. 1007–1010, https://doi.org/10.1130/G35924.1

Cassel, E. J., Smith, M. E., and Jicha, B. R., 2018, The impact of slab rollback on Earth's surface: Uplift and extension in the hinterland of the North American Cordillera: Geophysical Research Letters, v. 45, n. 20, p. 10996-11004, https://doi.org/10.1029/2018GL079887

Caves, J. K., Sjostrom, D. J., Mix, H. T., Winnick, M. J., and Chamberlain, C. P., 2014, Aridification of Central Asia and uplift of the Altai and Hangay Mountains, Mongolia: Stable isotope evidence: American journal of science, v. 314, n. 8, p. 1171–1201, https://doi.org/10.2475/08.2014.01

Caves, J. K., Winnick, M. J., Graham, S. A., Sjostrom, D. J., Mulch, A., and Chamberlain, C. P., 2015, Role of the westerlies in Central Asia climate over the Cenozoic: Earth and planetary science letters, v. 428, p. 33–43, https://doi.org/10.1016/j.epsl.2015.07.023

Caves, J. K., Moragne, D. Y., Ibarra, D. E., Bayshashov, B. U., Gao, Y., Jones, M. M., Zhamangara, A., Arzhannikova, A. V., Arzhannikov, S. G., and Chamberlain, C. P., 2016, The Neogene de-greening of central Asia: Geology, v. 44, n. 11, p. 887–890, https://doi.org/10.1130/G38267.1

Caves, J. K., Bayshashov, B. U., Zhamangara, A., Ritch, A. J., Ibarra, D. E., Sjostrom, D. J., Mix, H. T., Winnick, M. J., and Chamberlain, C. P., 2017, Late Miocene Uplift of the Tian Shan and Altai and Reorganization of Central Asia Climate: GSA Today, v.27, n. 2, p. 19–26, https://doi.org/10.1130/GSATG305A.1

Caves Rugenstein, J. K., and Chamberlain, C. P., 2018, The evolution of hydroclimate in Asia over the Cenozoic: A stable-isotope perspective: Earth-Science Reviews, v. 185, p. 1129–1156, https://doi.org/10.1016/j.earscirev.2018.09.003

Cerling, T. E., 1984, The stable isotopic composition of modern soil carbonate and its relationship to climate: Earth and Planetary Science Letters, v. 71, n. 2, p. 229–240, https://doi.org/10.1016/0012-821X(84)90089-X

Cerling, T. E. 1999, Stable Carbon Isotopes in Palaeosol Carbonates, *in* Thiry, M., and Simon-Coinçon, R., editors, Palaeoweathering, Palaeosurfaces and Related Continental Deposits: Oxford, United Kingdom, Blackwell Publishing Ltd., p. 43–60, https://doi.org/10.1002/9781444304190.ch2

Cerling, T. E., Wang, Y., and Quade, J., 1993, Expansion of C4 ecosystems as an indicator of global ecological change in the late Miocene: Nature, v. 361, p. 344–345, https://doi.org/10.1038/361344a0

Chamberlain, C. P., Mix, H. T., Mulch, A., Hren, M. T., Kent-Corson, M. L., Davis, S. J., Horton, T. W., and Graham, S. A., 2012, The Cenozoic climatic and topographic evolution of the western North American Cordillera: American journal of science, v. 312, n. 2, p. 213–262, https://doi.org/10.2475/02.2012.05

Chamberlain, C. P., Winnick, M. J., Mix, H. T., Chamberlain, S. D., and Maher, K., 2014, The impact of neogene grassland expansion and aridification on the isotopic composition of continental precipitation: Global Biogeochemical Cycles, v. 28, n. 9, p. 992–1004, https://doi.org/10.1002/2014GB004822

Chamberlain, C. P., Ibarra, D. E., Lloyd, M. K., Kukla, T., Sjostrom, D., Gao, Y., and Sharp, Z. D., 2020, Triple oxygen isotopes of meteoric hydrothermal systems – implications for palaeoaltimetry: Geochemical Perspectives Letters, v. 15, p. 6–9, https://doi.org/10.7185/geochemlet.2026

Charreau, J., Kent-Corson, M. L., Barrier, L., Augier, R., Ritts, B. D., Chen, Y., France-Lannord, C., and Guilmette, C., 2012, A high-resolution stable isotopic record from the Junggar Basin (NW China): Implications for the paleotopographic evolution of the Tianshan Mountains: Earth and Planetary Science Letters, v. 341–344, p. 158–169, https://doi.org/10.1016/j.epsl.2012.05.033

Clyde, W. C., Ting, S., Snell, K. E., Bowen, G. J., Tong, Y., Koch, P. L., Li, Q., and Wang, Y., 2010, New paleomagnetic and stable-isotope results from the nanxiong basin, China: Implications for the K/T boundary and the timing of Paleocene mammalian turnover: The Journal of Geology, v. 118, n. 2, p. 131–143, https://doi.org/10.1086/649893

Comas-Bru, L., Rehfeld, K., Roesch, C., Amirnezhad-Mozhdehi, S., Harrison, S. P., Atsawawaranunt, K., Ahmad, S. M., Brahim, Y. A., Baker, A., Bosomworth, M., Breitenbach, S. F. M., Burstyn, Y., Columbu, A., Deininger, M., Demény, A., Dixon, B., Fohlmeister, J., Hatvani, I. G., Hu, J., Kaushal, N., Kern, Z., Labuhn, I., Lechleitner, F. A., Lorrey, A., Martrat, B., Novello, V. F., Oster, J., Pérez-Mejías, C., Scholz, D., Scroxton, N., Sinha, N., Ward, B. M., Warken, S., and Zhang, H., 2020, SISALv2: a comprehensive speleothem isotope database with multiple age–depth models: Earth System Science Data, v. 12, p. 2579–2606, https://doi.org/10.5194/essd-12-2579-2020

Criss, R. E., and Taylor, H. P., 1983, An $^{18}O/^{16}O$ and D/H Study of Tertiary Hydrothermal Systems in the Southern Half of the Idaho Batholith: Geological Society of America Bulletin, v. 94, n. 5, p. 640–63, https://doi.org/10.1130/0016-7606(1983)94<640:AOADSO>2.0.CO;2

Crowley, B. E., Koch, P. L., and Davis, E. B., 2008, Stable Isotope Constraints on the Elevation History of the Sierra Nevada Mountains, California: Geological Society of America Bulletin, v. 120, n. 5–6, p. 588–598, https://doi.org/10.1130/B26254.1

Csonka, D., Bradák, B., Barta, G., Szeberényi, J., Novothny, Á., Végh, T., Süle, G. T., and Horváth, E., 2020, A multi-proxy study on polygenetic middle-to late pleistocene paleosols in the Hévízgyörk loess-paleosol sequence (Hungary): Quaternary International: the journal of the International Union for Quaternary Research, v. 552, p. 25–35, https://doi.org/10.1016/j.quaint.2019.07.021

Currie, B. S., Rowley, D. B., and Tabor, N. J., 2005, Middle Miocene Paleoaltimetry of Southern Tibet: Implications for the Role of Mantle Thickening and Delamination in the Himalayan Orogen: Geology, v. 33, n. 3, p. 181–184, https://doi.org/10.1130/G21170.1

Currie, B. S., Polissar, P. J., Rowley, D. B., Ingalls, M., Li, S., Olack, G., and Freeman, K. H., 2016, Multiproxy paleoaltimetry of the Late Oligocene-Pliocene Oiyug Basin, southern Tibet: American Journal of Science, v. 316, n. 5, p. 401–436, https://doi.org/10.2475/05.2016.01

Cyr, A. J., Currie, B. S., and Rowley, D. B., 2005, Geochemical evaluation of fenghuoshan group lacustrine carbonates, north-central Tibet: Implications for the paleoaltimetry of the Eocene Tibetan plateau: The journal of geology, v. 113, n. 5, p. 517–533, https://doi.org/10.1086/431907

Da, J., Zhang, Y. G., Li, G., Meng, X., and Ji, J., 2019, Low CO2 levels of the entire Pleistocene epoch: Nature communications, v. 10, p. 4342, https://doi.org/10.1038/s41467-019-12357-5

Davidson, G. R., 1995, The stable isotopic composition and measurement of carbon in soil CO_2: Geochimica et Cosmochimica Acta, v. 59, n. 12, p. 2485–2489, https://doi.org/10.1016/0016-7037(95)00143-3

Davis, S. J., Wiegand, B. A., Carroll, A. R., and Chamberlain, C. P., 2008, The effect of drainage reorganization on paleoaltimetry studies: An example from the Paleogene Laramide foreland: Earth and Planetary Science Letters, v. 275, n. 3–4, p. 258–268, https://doi.org/10.1016/j.epsl.2008.08.009

Davis, S. J., Mix, H. T., Wiegand, B. A., Carroll, A. R., and Chamberlain, C. P., 2009a, Synorogenic evolution of large-scale drainage patterns: Isotope paleohydrology of sequential Laramide basins: American Journal of Science, v. 309, n. 7, p. 549–602, https://doi.org/10.2475/07.2009.02

Davis, S. J., Mulch, A., Carroll, A. R., Horton, T. W., and Chamberlain, C. P., 2009b, Paleogene landscape evolution of the central North American Cordillera: Developing topography and hydrology in the

Laramide foreland: Geological Society of America Bulletin, v. 121, n. 1–2, p. 100–116, https://doi.org/10.1130/B26308.1

Dean, J. R., Jones, M. D., Leng, M. J., Noble, S. R., Metcalfe, S. E., Sloane, H. J., Sahy, D., Eastwood, W. J., and Roberts, C. N., 2015, Eastern Mediterranean hydroclimate over the late glacial and Holocene, reconstructed from the sediments of Nar lake, central Turkey, using stable isotopes and carbonate mineralogy: Quaternary Science Reviews, v. 124, p. 162–174, https://doi.org/10.1016/j.quascirev.2015.07.023

DeCelles, P. G., Quade, J., Kapp, P., Fan, M., Dettman, D. L., and Ding, L., 2007, High and dry in central Tibet during the Late Oligocene: Earth and planetary Science Letters, v. 253, n. 3–4, p. 389–401, https://doi.org/10.1016/j.epsl.2006.11.001

DeCelles, P. G., Kapp, P., Quade, J., and Gehrels, G. E., 2011, Oligocene-Miocene Kailas basin, southwestern Tibet: Record of postcollisional upper-plate extension in the Indus-Yarlung suture zone: Geological Society of America Bulletin, v. 123, n. 7–8, p. 1337–1362, https://doi.org/10.1130/B30258.1

Dee, S., Emile-Geay, J., Evans, M. N., Allam, A., Steig, E. J., and Thompson, D. M., 2015a, PRYSM: An open-source framework for PRoxY System Modeling, with applications to oxygen-isotope systems: Journal of Advances in Modeling Earth Systems, v. 7, n. 3, p. 1220–47, https://doi.org/10.1002/2015MS000447

Dee, S., Noone, D., Buenning, N., Emile-Geay, J., and Zhou, Y., 2015b, SPEEDY-IER: A fast atmospheric GCM with water isotope physics: Journal of Geophysical Research: Atmospheres, v. 120, n. 1, p. 73–91, https://doi.org/10.1002/2014JD022194

Dee, S. G., Russell, J. M., Morrill, C., Chen, Z., and Neary, A., 2018, PRYSM v2.0: A proxy system model for lacustrine archives: Paleoceanography and Paleoclimatology, v. 33, n. 11, p. 1250–1269, https://doi.org/10.1029/2018PA003413

Dettman, D. L., and Lohmann, K. C., 2000, Oxygen isotope evidence for high-altitude snow in the Laramide Rocky Mountains of North America during the Late Cretaceous and Paleogene, Geology, v. 28, v. 3, p. 243–246, https://doi.org/10.1130/0091-7613(2000)28<243:OIEFHS>2.0.CO;2

Dettman, D. L., Kohn, M. J., Quade, J., Ryerson, F. J., Ojha, T. P., and Hamidullah, S., 2001, Seasonal stable isotope evidence for a strong Asian monsoon throughout the past 10.7 m.y: Geology, v. 29, n. 1, p. 31–34, https://doi.org/10.1130/0091-7613(2001)029<0031:SSIEFA>2.0.CO;2

Dettman, D. L., Fang, X., Garzione, C. N., and Li, J., 2003, Uplift-driven climate change at 12 Ma: a long δ18O record from the NE margin of the Tibetan plateau: Earth and Planetary Science Letters, v. 214, n. 1–2, p. 267–277, https://doi.org/10.1016/S0012-821X(03)00383-2

Ding, Z. L., and Yang, S. L., 2000, C_3/C_4 vegetation evolution over the last 7.0 Myr in the Chinese Loess Plateau: evidence from pedogenic carbonate $\delta^{13}C$: Palaeogeography, Palaeoclimatology, Palaeoecology, v. 160, n. 3–4, p. 291–299, https://doi.org/10.1016/S0031-0182(00)00076-6

Ding, L., Xu, Q., Yue, Y., Wang, H., Cai, F., and Li, S., 2014, The Andean-type gangdese mountains: Paleoelevation record from the Paleocene–Eocene linzhou basin: Earth and Planetary Science Letters, v. 392, p. 250–264, https://doi.org/10.1016/j.epsl.2014.01.045

Doebbert, A. C., Carroll, A. R., Mulch, A., Chetel, L. M., and Chamberlain, C. P., 2010, Geomorphic controls on lacustrine isotopic compositions: Evidence from the Laney Member, Green River Formation, Wyoming: Geological Society of America Bulletin, v. 122, n. 1–2, p. 236–252, https://doi.org/10.1130/B26522.1

Domingo, L., Koch, P. L., Hernández Fernández, M., Fox, D. L., Domingo, M. S., and Alberdi, M. T., 2013, Late Neogene and early Quaternary paleoenvironmental and paleoclimatic conditions in southwestern Europe: Isotopic analyses on mammalian taxa: PloS ONE, v. 8, n. 5, p. e63739, https://doi.org/10.1371/journal.pone.0063739

Dong, J., Liu, Z., An, Z., Liu, W., Zhou, W., Qiang, X., and Lu, F., 2018, Mid-Miocene C_4 expansion on the Chinese Loess Plateau under an enhanced Asian summer monsoon: Journal of Asian Earth Sciences, v. 158, p. 153–159, https://doi.org/10.1016/j.jseaes.2018.02.014

Dzombak, R. M., Midttun, N. C., Stein, R. A., and Sheldon, N. D., 2021, Incorporating lateral variability and extent of paleosols into proxy uncertainty: Palaeogeography, Palaeoclimatology, Palaeoecology, v. 582, p. 110641, https://doi.org/10.1016/j.palaeo.2021.110641

Ekart, D. D., Cerling, T. E., Montañez, I. P., and Tabor, N. J., 1999, A 400 Million Year Carbon Isotope Record of Pedogenic Carbonate: Implications for Paleoatmospheric Carbon Dioxide: American Journal of Science, v. 299, n. 10, p. 805–27, https://doi.org/10.2475/ajs.299.10.805

Eren, M., 2011, Stable isotope geochemistry of Quaternary calcretes in the Mersin area, southern Turkey – A comparison and implications for their origin: Geochemistry, v. 71, n. 1, p. 31–37, https://doi.org/10.1016/j.chemer.2010.12.002

Evans, M. N., Tolwinski-Ward, S. E., Thompson, D. M., and Anchukaitis, K. J., 2013, Applications of proxy system modeling in high resolution paleoclimatology: Quaternary Science Reviews, v. 76, p. 16–28, https://doi.org/10.1016/j.quascirev.2013.05.024

Fan, M., and Dettman, D. L., 2009, Late Paleocene high Laramide ranges in northeast Wyoming: Oxygen isotope study of ancient river water: Earth and Planetary Science Letters, v. 286, n. 1–2, p. 110–121, https://doi.org/10.1016/j.epsl.2009.06.024

Fan, M., DeCelles, P.G., Gehrels, G.E., Dettman, D.L., Quade, J., and Peyton, S.L., 2011, Sedimentology, detrital zircon geochronology, and stable isotope geochemistry of the lower Eocene strata in the Wind River Basin, central Wyoming: Geological Society of America Bulletin, v. 123, n. 5–6, p. 979–96, https://doi.org/10.1130/B30235.1

Fan, M., Heller, P., Allen, S. D., and Hough, B. G., 2014a, Middle Cenozoic Uplift and Concomitant Drying in the Central Rocky Mountains and Adjacent Great Plains: Geology, v. 42, n. 6, p. 547–50, https://doi.org/10.1130/G35444.1

Fan, M., Hough, B. G., and Passey, B. H., 2014b, Middle to Late Cenozoic Cooling and High Topography in the Central Rocky Mountains: Constraints from Clumped Isotope Geochemistry: Earth and Planetary Science Letters, v. 408, p. 35–47, https://doi.org/10.1016/j.epsl.2014.09.050
Fan, M., Constenius, K. N., and Dettman, D. L., 2017, Prolonged high relief in the northern Cordilleran orogenic front during middle and late Eocene extension based on stable isotope paleoaltimetry: Earth and Planetary Science Letters, v. 457, p. 376–384, https://doi.org/10.1016/j.epsl.2016.10.038
Fan, M., Ayyash, S. A., Tripati, A., Passey, B. H., and Griffith, E. M., 2018, Terrestrial cooling and changes in hydroclimate in the continental interior of the United States across the Eocene-Oligocene boundary: Geological Society of America Bulletin, v. 130, n. 7–8, p. 1073–1084, https://doi.org/10.1130/B31732.1
Fan, M., Constenius, K. N., Phillips, R. F., and Dettman, D. L., 2021, Late Paleogene paleotopographic evolution of the northern Cordilleran orogenic front: Implications for demise of the orogen: Geological Society of America Bulletin, https://doi.org/10.1130/B35919.1
Foreman, B. Z., Fricke, H. C., Lohmann, K. C., and Rogers, R. R., 2011, Reconstructing paleocatchments by integrating stable isotope records, sedimentology, and taphonomy: A late cretaceous case study (Montana, United States): PALAIOS, v. 26, n. 9, p. 545–554, https://doi.org/10.2110/palo.2010.p10-133r
Foreman, B. Z., Roberts, E. M., Tapanila, L., Ratigan, D., and Sullivan, P., 2015, Stable isotopic insights into paleoclimatic conditions and alluvial depositional processes in the Kaiparowits Formation (Campanian, south-central Utah, U.S.A.): Cretaceous Research, v. 56, p. 180–192, https://doi.org/10.1016/j.cretres.2015.05.001
Fox, D. L., and Koch, P. L., 2003, Tertiary history of C4 biomass in the Great Plains, USA: Geology, v. 31, n. 9, p. 809–812, https://doi.org/10.1130/G19580.1
Fox, D., and Koch, P. L., 2004, Carbon and oxygen isotopic variability in Neogene paleosol carbonates: constraints on the evolution of the C_4-grasslands of the Great Plains, USA: Palaeogeography, Palaeoclimatology, Palaeoecology, v. 207, n. 3–4, p. 305–329, https://doi.org/10.1016/S0031-0182(04)00045-8
Fox, D. L., Honey, J. G., Martin, R. A., and Pelaez-Campomanes, P., 2012, Pedogenic carbonate stable isotope record of environmental change during the Neogene in the southern Great Plains, southwest Kansas, USA: Carbon isotopes and the evolution of C_4-dominated grasslands: Geological Society of America bulletin, v. 124, n. 3–4, p. 444–462, https://doi.org/10.1130/B30401.1
Fox, D. L., Pau, S., Taylor, L., Strömberg, C. A. E., Osborne, C. P., Bradshaw, C., Conn, S., Beerling, D. J., and Still, C. J., 2018, Climatic controls on C4 grassland distributions during the Neogene: A model-data comparison: Frontiers in Ecology and Evolution, v. 6, p. 147, https://doi.org/10.3389/fevo.2018.00147
Fricke, H. C., 2003. Investigation of early Eocene water-vapor transport and paleoelevation using oxygen isotope data from geographically widespread mammal remains: Geological Society of America Bulletin, v. 115, n. 9, p. 1088–1096, https://doi.org/10.1130/B25249.1
Fricke, H. C., and Wing, S. L., 2004, Oxygen isotope and paleobotanical estimates of temperature and $\delta^{18}O$-latitude gradients over North America during the early Eocene: American Journal of Science, v. 304, n. 7, p. 612–635, https://doi.org/10.2475/ajs.304.7.612
Fricke, H. C., Clyde, W. C., O'Neil, J. R., and Gingerich, P. D., 1998, Evidence for rapid climate change in North America during the latest Paleocene thermal maximum: oxygen isotope compositions of biogenic phosphate from the Bighorn Basin (Wyoming): Earth and Planetary Science Letters, v. 160, n. 1–2, p. 193–208, https://doi.org/10.1016/S0012-821X(98)00088-0
Fricke, H. C., Rogers, R. R., Backlund, R., Dwyer, C. N., and Echt, S., 2008, Preservation of primary stable isotope signals in dinosaur remains, and environmental gradients of the Late Cretaceous of Montana and Alberta: Palaeogeography, Palaeoclimatology, Palaeoecology, v. 266, n. 1–2, p. 13–27, https://doi.org/10.1016/j.palaeo.2008.03.030
Fricke, H. C., Foreman, B. Z., and Sewall, J. O., 2010, Integrated climate model-oxygen isotope evidence for a North American monsoon during the Late Cretaceous: Earth and Planetary Science Letters, v. 289, n. 1–2, p. 11–21, https://doi.org/10.1016/j.epsl.2009.10.018
Gallant, C. E., Candy, I., van den Bogaard, P., Silva, B. N., and Turner, E., 2014, Stable isotopic evidence for Middle Pleistocene environmental change from a loess-paleosol sequence: Kärlich, Germany: Middle Pleistocene environmental change, Kärlich, Germany: Boreas, v. 43, n. 4, p. 818–833, https://doi.org/10.1111/bor.12065
Gao, Y., Ibarra, D. E., Caves Rugenstein, J. K., Chen, J., Kukla, T., Methner, K., Gao, Y., Huang, H., Lin, Z., Zhang, L., Xi, D., Wu, H., Carroll, A. R., Graham, S. A., Chamberlain, C. P., and Wang, C., 2021, Terrestrial climate in mid-latitude East Asia from the latest Cretaceous to the earliest Paleogene: A multiproxy record from the Songliao Basin in northeastern China: Earth-Science Reviews, v. 216, p. 103572, https://doi.org/10.1016/j.earscirev.2021.103572
Gat, G. R., 1996, Oxygen and Hydrogen Isotopes in the Hydrologic Cycle: Annual Review of Earth and Planetary Sciences, v. 24, p. 225–262, https://doi.org/10.1146/annurev.earth.24.1.225
Garzione, C. N., Dettman, D. L., Quade, J., DeCelles, P. G., and Butler, R. F., 2000, High times on the Tibetan Plateau: Paleoelevation of the Thakkhola graben, Nepal: Geology, v. 28, n. 4, p. 339–342, https://doi.org/10.1130/0091-7613(2000)28<339:HTOTTP>2.0.CO;2
Gébelin, A., Mulch, A., Teyssier, C., Chamberlain, C. P., and Heizler, M., 2012, Coupled basin-detachment systems as paleoaltimetry archives of the western North American Cordillera: Earth and Planetary Science Letters, v. 335–336, p. 36–47, https://doi.org/10.1016/j.epsl.2012.04.029
Genty, D., Blamart, D., Ouahdi, R., Gilmour, M., Baker, A., Jouzel, J., and Van-Exter, S., 2003, Precise dating of Dansgaard-Oeschger climate oscillations in western Europe from stalagmite data: Nature, v. 421, p. 833–837, https://doi.org/10.1038/nature01391

Ghosh, P., Padia, J. T., and Mohindra, R., 2004, Stable isotopic studies of palaeosol sediment from Upper Siwalik of Himachal Himalaya: evidence for high monsoonal intensity during late Miocene? Palaeogeography, Palaeoclimatology, Palaeoecology, v. 206, n. 1–2, p. 103–114, https://doi.org/10.1016/j.palaeo.2004.01.014

Godfrey, C., Fan, M., Jesmok, G., Upadhyay, D., and Tripati, A., 2018, Petrography and stable isotope geochemistry of Oligocene-Miocene continental carbonates in south Texas: Implications for paleoclimate and paleoenvironment near sea-level: Sedimentary Geology, v. 367, p. 69–83, https://doi.org/10.1016/j.sedgeo.2018.02.006

Harris, E. B., Kohn, M. J., and Strömberg, C. A. E., 2020, Stable isotope compositions of herbivore teeth indicate climatic stability leading into the mid-Miocene Climatic Optimum, in Idaho, U.S.A: Palaeogeography, Palaeoclimatology, Palaeoecology, v. 546, p. 109610, https://doi.org/10.1016/j.palaeo.2020.109610

Harzhauser, M., Latal, C., and Piller, W. E., 2007, The stable isotope archive of Lake Pannon as a mirror of Late Miocene climate change: Palaeogeography, Palaeoclimatology, Palaeoecology, v. 249, n. 3–4, p. 335–350, https://doi.org/10.1016/j.palaeo.2007.02.006

Harzhauser, M., Mandic, O., Latal, C., and Kern, A., 2012, Stable isotope composition of the Miocene Dinaride Lake System deduced from its endemic mollusc fauna: Hydrobiologia, v. 682, n. 1, p. 27–46, https://doi.org/10.1007/s10750-011-0618-3

Heitmann, E. O., Ji, S., Nie, J., and Breecker, D. O., 2017, Orbitally-paced variations of water availability in the SE Asian Monsoon region following the Miocene Climate Transition: Earth and Planetary Science Letters, v. 474, p. 272–282, https://doi.org/10.1016/j.epsl.2017.06.006

Hellwig, A., Voigt, S., Mulch, A., Frisch, K., Bartenstein, A., Pross, J., Gerdes, A., and Voigt, T., 2018, Late Oligocene to early Miocene humidity change recorded in terrestrial sequences in the Ili Basin (south-eastern Kazakhstan, Central Asia): Sedimentology, v. 65, n. 2, p. 517–539, https://doi.org/10.1111/sed.12390

Hendricks, M. B., DePaolo, D. J., and Cohen, R. C., 2000, Space and time variation of $\delta^{18}O$ and δD in precipitation: Can paleotemperature be estimated from ice cores?: Global Biogeochemical Cycles, v. 14, n. 3, p. 851–861, https://doi.org/10.1029/1999GB001198

Hofman-Kamińska, E., Bocherens, H., Borowik, T., Drucker, D. G., and Kowalczyk, R., 2018, Stable isotope signatures of large herbivore foraging habitats across Europe: PloS One, v. 13, n. 1, p. e0190723, https://doi.org/10.1371/journal.pone.0190723

Hoke, G. D., Liu-Zeng, J., Hren, M. T., Wissink, G. K., and Garzione, C. N., 2014, Stable isotopes reveal high southeast Tibetan Plateau margin since the Paleogene: Earth and Planetary Science Letters, v. 394, p. 270–278, https://doi.org/10.1016/j.epsl.2014.03.007

Honegger, L., Adatte, T., Spangenberg, J. E., Rugenstein, J. K. C., Poyatos-Moré, M., Puigdefàbregas, C., Chanvry, E., Clark, J., Fildani, A., Verrechia, E., Kouzmanov, K., Harlaux, M., and Castelltort, S., 2020, Alluvial record of an early Eocene hyperthermal within the Castissent Formation, the Pyrenees, Spain: Climate of the Past, v. 16, n. 1, p. 227–243, https://doi.org/10.5194/cp-16-227-2020

Horton, T. W., and Chamberlain, C. P., 2006, Stable isotopic evidence for Neogene surface downdrop in the central Basin and Range Province: Geological Society of America Bulletin, v. 118, n. 3–4, p. 475–90, https://doi.org/10.1130/B25808

Horton, T. W., Sjostrom, D. J., Abruzzese, M. J., Poage, M. A., Waldbauer, J. R., Hren, M., Wooden, J., and Chamberlain, C. P., 2004, Spatial and Temporal Variation of Cenozoic Surface Elevation in the Great Basin and Sierra Nevada: American Journal of Science v. 304, n. 650, p. 862–88, https://doi.org/10.2475/ajs.304.10.862

Hough, B. G., Garzione, C. N., Wang, Z., Lease, R. O., Burbank, D. W., and Yuan, D., 2011, Stable isotope evidence for topographic growth and basin segmentation: Implications for the evolution of the NE Tibetan Plateau: Geological Society of America Bulletin, v. 123, n. 1–2, 168–185, https://doi.org/10.1130/B30090.1

Hough, B. G., Fan, M., and Passey, B. H., 2014, Calibration of the Clumped Isotope Geothermometer in Soil Carbonate in Wyoming and Nebraska, USA: Implications for Paleoelevation and Paleoclimate Reconstruction: Earth and Planetary Science Letters, v. 391, p. 110–20, https://doi.org/10.1016/j.epsl.2014.01.008

Hren, M. T., Pagani, M., Erwin, D. M., and Brandon, M., 2010, Biomarker reconstruction of the early Eocene paleotopography and paleoclimate of the northern Sierra Nevada: Geology, v. 38, n. 1, p. 7–10, https://doi.org/10.1130/G30215.1

Huntington, K. W., Eiler, J. M., Affek, H. P., Guo, W., Bonifacie, M., Yeung, L. Y., Thiagarajan, N., Passey, B., Tripati, A., Daëron, M., and Came, R., 2009, Methods and limitations of "clumped" CO2 isotope (Δ_{47}) analysis by gas-source isotope ratio mass spectrometry: Journal of Mass Spectrometry, v. 44, n. 9, p. 1318–1329, https://doi.org/10.1002/jms.1614

Huntington, K. W., Wernicke, B. P., and Eiler, J. M., 2010, Influence of climate change and uplift on Colorado Plateau paleotemperatures from carbonate clumped isotope thermometry:Tectonics, v. 29, n. 3, p. 2009TC002449, https://doi.org/10.1029/2009TC002449

Huntington, K. W., Budd, D. A., Wernicke, B. P., and Eiler, J. M., 2011, Use of clumped-isotope thermometry to constrain the crystallization temperature of diagenetic calcite: Journal of Sedimentary Research, v. 81, n. 9, p. 656–69, https://doi.org/10.2110/jsr.2011.51

Huyghe, D., Emmanuel, L., Renard, M., Lartaud, F., Génot, P., Riveline, J., and Merle, D., 2017, Significance of shallow-marine and non-marine algae stable isotope ($\delta^{18}O$) compositions over long periods: Example from the Palaeogene of the Paris Basin: Palaeogeography, Palaeoclimatology, Palaeoecology, v. 485, p. 247–259, https://doi.org/10.1016/j.palaeo.2017.06.017

Hyland, E. G., and Sheldon, N. D., 2013, Coupled CO_2-climate response during the Early Eocene Climatic Optimum: Palaeogeography, Palaeoclimatology, Palaeoecology, v. 369, p. 125–135, https://doi.org/10.1016/j.palaeo.2012.10.011

Hyland, E., Sheldon, N. D., and Fan, M., 2013, Terrestrial paleoenvironmental reconstructions indicate transient peak warming during the early Eocene climatic optimum: Geological Society of America Bulletin, v. 125, n. 7–8, p. 1338–1348, https://doi.org/10.1130/B30761.1

Ibarra, D. E., and Chamberlain, C. P., 2015, Quantifying closed-basin lake temperature and hydrology by inversion of oxygen isotope and trace element paleoclimate records: American journal of science, v. 315, n. 9, p. 781–808, https://doi.org/10.2475/09.2015.01

Ibarra, D. E., Kukla, T., Methner, K. A., Mulch, A., and Chamberlain, C. P., 2021, Reconstructing past elevations from triple oxygen isotopes of lacustrine chert: Application to the Eocene Nevadaplano, Elko Basin, Nevada, United States: Frontiers in Earth Science, v. 9, p. 628868, https://doi.org/10.3389/feart.2021.628868

Ingalls, M., Rowley, D., Olack, G., Currie, B., Li, S., Schmidt, J., Tremblay, M., Polissar, P., Shuster, D. L., Lin, D., and Colman, A., 2018, Paleocene to Pliocene low-latitude, high-elevation basins of southern Tibet: Implications for tectonic models of India-Asia collision, Cenozoic climate, and geochemical weathering: Geological Society of America Bulletin, v. 130, n 1–2, p. 307–330, https://doi.org/10.1130/B31723.1

Jensen, T. Z. T., Sjöström, A., Fischer, A., Rosengren, E., Lanigan, L. T., Bennike, O., Richter, K. K., Gron, K. J., Mackie, M., Mortensen, M. F., Sørensen, L., Chivall, D., Iversen, K. H., and Taurozzi, A. J. and others, 2020, An integrated analysis of Maglemose bone points reframes the Early Mesolithic of Southern Scandinavia: Scientific reports, v. 10, n. 1, p. 17244, https://doi.org/10.1038/s41598-020-74258-8

Ji, S., Nie, J., Lechler, A., Huntington, K. W., Heitmann, E. O., and Breecker, D. O., 2018, A symmetrical CO_2 peak and asymmetrical climate change during the middle Miocene: Earth and Planetary Science Letters, v. 499, p. 134–144, https://doi.org/10.1016/j.epsl.2018.07.011

Jiang, W., Peng, S., Hao, Q., and Liu, T., 2002, Carbon isotopic records in paleosols over the Pliocene in Northern China: Implication on vegetation development and Tibetan uplift: Chinese Science Bulletin, v. 47, n. 8, p. 687, https://doi.org/10.1360/02tb9156

Jolivet, M., and Boulvais, P., 2021, Global significance of oxygen and carbon isotope compositions of pedogenic carbonates since the Cretaceous: Geoscience Frontiers, v. 12, n. 4, p. 101132, https://doi.org/10.1016/j.gsf.2020.12.012

Kaakinen, A., Sonninen, E., and Lunkka, J. P., 2006, Stable isotope record in paleosol carbonates from the Chinese Loess Plateau: Implications for late Neogene paleoclimate and paleovegetation: Palaeogeography, Palaeoclimatology, Palaeoecology, v. 237, n. 2–4, p. 359–369, https://doi.org/10.1016/j.palaeo.2005.12.011

Kaufman, D., McKay, N., Routson, C., Erb, M., Davis, B., Heiri, O., Jaccard, S., Tierney, J., Dätwyler, C., Axford, Y., Brussel, T., Cartapanis, O., Chase, B., Dawson, A., de Vernal, A., Engels, S., Jonkers, L., and Marsicek, J., and others, 2020, A global database of Holocene paleotemperature records: Scientific data, v. 7, p. 115, https://doi.org/10.1038/s41597-020-0445-3

Kelson, J. R., Watford, D., Bataille, C., Huntington, K. W., Hyland, E., and Bowen, G. J., 2018, Warm terrestrial subtropics during the Paleocene and Eocene: Carbonate clumped isotope (Δ_{47}) evidence from the Tornillo basin, Texas (USA): Paleoceanography and Paleoclimatology, v. 33, n. 11, p. 1230–1249, https://doi.org/10.1029/2018PA003391

Kent-Corson, M. L., Sherman, L. S., Mulch, A., and Chamberlain, C. P., 2006, Cenozoic topographic and climatic response to changing tectonic boundary conditions in Western North America: Earth and Planetary Science Letters, v. 252, n. 3–4, p. 453–466, https://doi.org/10.1016/j.epsl.2006.09.049

Kent-Corson, M. L., Ritts, B. D., Zhuang, G., Bovet, P. M., Graham, S. A., and Page Chamberlain, C., 2009, Stable isotopic constraints on the tectonic, topographic, and climatic evolution of the northern margin of the Tibetan Plateau: Earth and Planetary Science Letters, v. 282, n. 1–4, p. 158–166, https://doi.org/10.1016/j.epsl.2009.03.011

Kent-Corson, M. L., Mulch, A., Graham, S. A., Carroll, A. R., Ritts, B. D., and Chamberlain, C. P., 2010, Diachronous isotopic and sedimentary responses to topographic change as indicators of mid-Eocene hydrologic reorganization in the western United States: Basin Research, v. 22, n. 6, p. 829–845, https://doi.org/10.1111/j.1365-2117.2009.00456.x

Kent-Corson, M. L., Barnosky, A. D., Mulch, A., Carrasco, M. A., and Chamberlain, C. P., 2013, Possible regional tectonic controls on mammalian evolution in western North America: Palaeogeography, Palaeoclimatology, Palaeoecology, v. 387, p. 17–26, https://doi.org/10.1016/j.palaeo.2013.07.014

Kluge, T., and Affek, H. P., 2012, Quantifying kinetic fractionation in Bunker Cave speleothems using Δ_{47}: Quaternary Science Reviews, v. 49, p. 82–94, https://doi.org/10.1016/j.quascirev.2012.06.013

Koch, P. L., Zachos, J. C., and Dettman, D. L., 1995, Stable isotope stratigraphy and paleoclimatology of the Paleogene Bighorn Basin (Wyoming, USA): Palaeogeography, Palaeoclimatology, Palaeoecology, v. 115, p. 61–89, https://doi.org/10.1016/0031-0182(94)00107-J

Koch, P. L., Clyde, W. C., Hepple, R. P., Fogel, M. L., Wing, S. L., and Zachos, J. C., 2003, Carbon and oxygen isotope records from Paleosols spanning the Paleocene-Eocene boundary, Bighorn Basin, Wyoming, *in* Wing, S. L., Gingerich, P. D., Schmitz, B., and Thomas, E., editors, Causes and consequences of globally warm climates in the early Paleogene: Geological Society of America, GSA Special Papers, v. 369, p. 49–64, https://doi.org/10.1130/0-8137-2369-8.49

Kocsis, L., Ozsvárt, P., Becker, D., Ziegler, R., Scherler, L., and Codrea, V., 2014, Orogeny forced terrestrial climate variation during the late Eocene–early Oligocene in Europe: Geology, v. 42, n. 8, p. 727–730, https://doi.org/10.1130/G35673.1

Kohn, M. J., and Cerling, T. E., 2002, Stable Isotope Compositions of Biological Apatite: Reviews in Mineralogy and Geochemistry, v. 48, n. 1, p. 455–88, https://doi.org/10.2138/rmg.2002.48.12

Kohn, M. J., and Law, J. M., 2006, Stable isotope chemistry of fossil bone as a new paleoclimate indicator: Geochimica et Cosmochimica Acta, v. 70, n. 4, p. 931–946, https://doi.org/10.1016/j.gca.2005.10.023

Kohn, M. J., Miselis, J. L., and Fremd, T. J., 2002, Oxygen isotope evidence for progressive uplift of the Cascade Range, Oregon: Earth and Planetary Science Letters, v. 204, n. 1–2, p. 151–165, https://doi.org/10.1016/S0012-821X(02)00961-5

Konecky, B. L., McKay, N. P., Churakova (Sidorova), O. V., Comas-Bru, L., Dassié, E. P., DeLong, K. L., Falster, G. M., Fischer, M. J., Jones, M. D., Jonkers, L., Kaufman, D. S., Leduc, G., Managave, S. R., Martrat, B., Managave, S. R., Martrat, B., Opel, T., Orsi, A. J., Partin, J. W., Sayani, H. R., Thomas, E. K., Thompson, D. M., Tyler, J. J., Abram, N. J., Atwood, A. R., Cartapanis, O., Conroy, J. L., Curran, M. A., Dee, S. G., Deininger, M., Divine, D. V., Kern, Z., Porter, T. J., Stevenson, S. L., and von Gunten, L., 2020, The Iso2k database: a global compilation of paleo-δ^{18}O and δ^{2}H records to aid understanding of Common Era climate: Earth System Science Data, v. 12, p. 2261–2288, https://doi.org/10.5194/essd-12-2261-2020

Kovács, J., Moravcová, M., Újvári, G., and Pintér, A. G., 2012, Reconstructing the paleoenvironment of East Central Europe in the Late Pleistocene using the oxygen and carbon isotopic signal of tooth in large mammal remains: Quaternary international: The Journal of the International Union for Quaternary Research, v. 276–277, p. 145–154, https://doi.org/10.1016/j.quaint.2012.04.009

Kovács, J., Szabó, P., Kocsis, L., Vennemann, T., Sabol, M., Gasparik, M., and Virág, A., 2015, Pliocene and Early Pleistocene paleoenvironmental conditions in the Pannonian Basin (Hungary, Slovakia): Stable isotope analyses of fossil proboscidean and perissodactyl teeth: Palaeogeography, Palaeoclimatology, Palaeoecology, v. 440, p. 455–466, https://doi.org/10.1016/j.palaeo.2015.09.019

Kovda, I., Mora, C. I., and Wilding, L. P., 2008, PaleoVertisols of the northwest Caucasus: (Micro)morphological, physical, chemical, and isotopic constraints on early to late Pleistocene climate: Journal of Plant Nutrition and Soil Science, v. 171, n. 4, p. 498–508, https://doi.org/10.1002/jpln.200700037

Küçükuysal, C., and Kapur, S., 2014, Mineralogical, geochemical and micromorphological evaluation of the Plio-Quaternary paleosols and calcretes from Karahamzall, Ankara (Central Turkey): Geologica Carpathica, v. 65, n. 3, p. 243–255, https://doi.org/10.2478/geoca-2014-0014

Kukla, T., Winnick, M. J., Maher, K., Ibarra, D. E., and Chamberlain, C. P., 2019, The sensitivity of terrestrial δ^{18} O gradients to hydroclimate evolution: Journal of Geophysical Research Atmospheres, v. 124, n. 2, p. 563–582, https://doi.org/10.1029/2018JD029571

Kukla, T., Ahlström, A., Maezumi, S. Y., Chevalier, M., Lu, Z., Winnick, M. J., and Chamberlain, C. P., 2021a, The resilience of Amazon tree cover to past and present drying: Global and Planetary Change, v. 202, p. 103520, https://doi.org/10.1016/j.gloplacha.2021.103520

Kukla, T., Ibarra, D. E., Rugenstein, J. K. C., Gooley, J. T., Mullins, C. E., Kramer, S., Moragne, D. Y., and Chamberlain, C. P., 2021b, High-resolution stable isotope paleotopography of the John Day region, Oregon, United States: Frontiers in Earth Science, v. 9, p. 635181, https://doi.org/10.3389/feart.2021.635181

Lacroix, B., and Niemi, N. A., 2019, Investigating the effect of burial histories on the clumped isotope thermometer: An example from the Green River and Washakie Basins, Wyoming: Geochimica et Cosmochimica Acta, v. 247, p. 40–58, https://doi.org/10.1016/j.gca.2018.12.016

Latorre, C., Quade, J., and McIntosh, W. C., 1997, The expansion of C4 grasses and global change in the late Miocene: Stable isotope evidence from the Americas: Earth and planetary science letters, v. 146, n. 1–2, p. 83–96, https://doi.org/10.1016/S0012-821X(96)00231-2

Leary, R. J., Quade, J., DeCelles, P. G., and Reynolds, A., 2017, Evidence from paleosols for low to moderate elevation of the India-Asia suture zone during mid-Cenozoic time: Geology, v. 45, n. 5, p.399–402, https://doi.org/10.1130/G38830.1

Lechler, A. R., and Niemi, N. A., 2011, Sedimentologic and isotopic constraints on the Paleogene paleogeography and paleotopography of the southern Sierra Nevada, California: Geology, v. 39, n. 4, p.379–382, https://doi.org/10.1130/G31535.1

Leone, G., Bonadonna, F., and Zanchetta, G., 2000, Stable isotope record in mollusca and pedogenic carbonate from Late Pliocene soils of Central Italy: Palaeogeography, Palaeoclimatology, Palaeoecology, v. 163, n. 3–4, p. 115–131, https://doi.org/10.1016/S0031-0182(00)00148-6

Licht, A., van Cappelle, M., Abels, H. A., Ladant, J.-B., Trabucho-Alexandre, J., France-Lanord, C., Donnadieu, Y., Vandenberghe, J., Rigaudier, T., Lécuyer, C., Terry, D. Jr, Adriaens, R., Boura, A., and Guo, Z., and others, 2014, Asian monsoons in a late Eocene greenhouse world: Nature, v. 513, n. 7519, p. 501–506, https://doi.org/10.1038/nature13704

Licht, A., Coster, P., Ocakoğlu, F., Campbell, C., Métais, G., Mulch, A., Taylor, M., Kappelman, J., and Beard, K. C., 2017a, Tectono-stratigraphy of the Orhaniye Basin, Turkey: Implications for collision chronology and Paleogene biogeography of central Anatolia: Journal of Asian Earth Sciences, v. 143, p. 45–58, https://doi.org/10.1016/j.jseaes.2017.03.033

Licht, A., Quade, J., Kowler, A., de los Santos, M., Hudson, A., Schauer, A., Huntington, K., Copeland, P., and Lawton, T., 2017b, Impact of the North American monsoon on isotope paleoaltimeters: Implications for the paleoaltimetry of the American southwest: American Journal of Science, v. 317, n. 1, p. 1–33, https://doi.org/10.2475/01.2017.01

Licht, A., Dupont-Nivet, G., Meijer, N., Caves Rugenstein, J., Schauer, A., Fiebig, J., Mulch, A., Hoorn, C., Barbolini, N., and Guo, Z., 2020, Decline of soil respiration in northeastern Tibet through the transition into the Oligocene icehouse: Palaeogeography, Palaeoclimatology, Palaeoecology, v. 560, p. 110016, https://doi.org/10.1016/j.palaeo.2020.110016

Li, B., Sun, D., Wang, X., Zhang, Y., Hu, W., Wang, F., Li, Z., Ma, Z., and Liang, B., 2016a, δ^{18}O and δ^{13}C records from a Cenozoic sedimentary sequence in the Lanzhou Basin, Northwestern China: Implications for palaeoenvironmental and palaeoecological changes: Journal of Asian Earth Sciences, v. 125, p. 22–36, https://doi.org/10.1016/j.jseaes.2016.05.010

Li, L., Garzione, C. N., Pullen, A., and Chang, H., 2016b, Early–middle Miocene topographic growth of the northern Tibetan Plateau: Stable isotope and sedimentation evidence from the southwestern Qaidam basin: Palaeogeography, Palaeoclimatology, Palaeoecology, v. 461, p. 201–213, https://doi.org/10.1016/j.palaeo.2016.08.025

Li, L., Fan, M., and Zhu, L., 2021, Early Oligocene surface uplift in southwestern Montana during the north American cordilleran extension: Tectonics, v. 40, n. 7, p. e2020TC006671, https://doi.org/10.1029/2020TC006671

Li, S., Currie, B. S., Rowley, D. B., and Ingalls, M., 2015, Cenozoic paleoaltimetry of the SE margin of the Tibetan Plateau: Constraints on the tectonic evolution of the region: Earth and Planetary Science Letters, V. 432, p. 415–424, https://doi.org/10.1016/j.epsl.2015.09.044

Liu, W., Liu, Z., An, Z., Sun, J., Chang, H., Wang, N., Dong, J., and Wang, H., 2014, Late Miocene episodic lakes in the arid Tarim Basin, western China: Proceedings of the National Academy of Sciences of the United States of America, v. 111, n. 46, p. 16292–16296, https://doi.org/10.1073/pnas.1410890111

Lüedecke, T., Mikes, T., Rojay, F.B., Cosca, M.A., and Mulch, A., 2013, Stable isotope-based reconstruction of Oligo-Miocene paleoenvironment and paleohydrology of Central Anatolian lake basins (Turkey): Turkish Journal of Earth Sciences, v. 22, n. 5, p.793–819, https://doi.org/10.3906/yer-1207-11

Lukens, W. E., Driese, S. G., Peppe, D. J., and Loudermilk, M., 2017, Sedimentology, stratigraphy, and paleoclimate at the late Miocene Coffee Ranch fossil site in the Texas Panhandle: Palaeogeography, Palaeoclimatology, Palaeoecology, v. 485, p. 361–376, https://doi.org/10.1016/j.palaeo.2017.06.026

Macaulay, E. A., Sobel, E. R., Mikolaichuk, A., Wack, M., Gilder, S. A., Mulch, A., Fortuna, A. B., Hynek, S., and Apayarov, F., 2016, The sedimentary record of the Issyk Kul basin, Kyrgyzstan: climatic and tectonic inferences: Basin Research, v. 28, n. 1, p. 57–80, https://doi.org/10.1111/bre.12098

Mack, G. H., and Cole, D. R., 2005, Geochemical model of $\delta^{18}O$ of pedogenic calcite versus latitude and its application to Cretaceous palaeoclimate: Sedimentary Geology, v. 174, n. 1–2, p. 115–122, https://doi.org/10.1016/j.sedgeo.2004.12.002

Mack, G. H., Cole, D. R., James, W. C., Giordano, T. H., and Salyards, S. L., 1994, Stable oxygen and carbon isotopes of pedogenic carbonate as indicators of Plio-Pleistocene paleoclimate in southern Rio Grande Rift, south-central New Mexico: American Journal of Science, v. 294, n. 5, p. 621–640, https://doi.org/10.2475/ajs.294.5.621

Matson, S. D., and Fox, D. L., 2010, Stable isotopic evidence for terrestrial latitudinal climate gradients in the Late Miocene of the Iberian Peninsula: Palaeogeography, Palaeoclimatology, Palaeoecology, v. 287, n. 1–4, p. 28–44, https://doi.org/10.1016/j.palaeo.2009.12.010

Matson, S. D., Rook, L., Oms, O., and Fox, D. L., 2012, Carbon isotopic record of terrestrial ecosystems spanning the Late Miocene extinction of Oreopithecus bambolii, Baccinello Basin (Tuscany, Italy): Journal of Human Evolution, v. 63, n. 1, p. 127–139, https://doi.org/10.1016/j.jhevol.2012.04.004

McFadden, R. R., Mulch, A., Teyssier, C., and Heizler, M., 2015, Eocene extension and meteoric fluid flow in the Wildhorse detachment, Pioneer metamorphic core complex, Idaho: Lithosphere, v. 7, n. 4, p. 355–66, https://doi.org/10.1130/L429.1

McLean, A., and Bershaw, J., 2021, Molecules to mountains: A multi-proxy investigation into ancient climate and topography of the Pacific Northwest, USA: Frontiers in Earth Science, v. 9, p.624961, https://doi.org/10.3389/feart.2021.624961

Meijers, M. J., Strauss, B. E., Özkaptan, M., Feinberg, J. M., Mulch, A., Whitney, D. L., and Kaymakçı, N., 2016, Age and paleoenvironmental reconstruction of partially remagnetized lacustrine sedimentary rocks (Oligocene Aktoprak basin, central Anatolia, Turkey): Geochemistry, Geophysics, Geosystems, v. 17, n. 3, p.914–939, https://doi.org/10.1002/2015GC006209

Meijers, M. J. M., Peynircioğlu, A. A., Cosca, M. A., Brocard, G. Y., Whitney, D. L., Langereis, C. G., and Mulch, A., 2018, Climate stability in central Anatolia during the Messinian Salinity Crisis: Palaeogeography, Palaeoclimatology, Palaeoecology, v. 498, p. 53–67, https://doi.org/10.1016/j.palaeo.2018.03.001

Methner, K., Mulch, A., Teyssier, C., Wells, M. L., Cosca, M. A., Gottardi, R., Gébelin, A., and Chamberlain, C. P., 2015, Eocene and Miocene extension, meteoric fluid infiltration, and core complex formation in the Great Basin (Raft River Mountains, Utah): Tectonics, v. 34, n. 4, p. 680–693, https://doi.org/10.1002/2014TC003766

Methner, K., Fiebig, J., Wacker, U., Umhoefer, P., Chamberlain, C. P., and Mulch, A., 2016a, Eocene-Oligocene proto-Cascades topography revealed by clumped (Δ_{47}) and oxygen isotope ($\delta^{18}O$) geochemistry (Chumstick Basin, WA, USA): Eo-Oligocene Proto-Cascades Topography: Tectonics, v. 35, n. 3, p. 546–564, https://doi.org/10.1002/2015TC003984

Methner, K., Mulch, A., Fiebig, J., Wacker, U., Gerdes, A., Graham, S. A., and Chamberlain, C. P., 2016b, Rapid Middle Eocene temperature change in western North America: Earth and Planetary Science Letters, v. 450, p. 132–139, https://doi.org/10.1016/j.epsl.2016.05.053

Methner, K., Campani, M., Fiebig, J., Löffler, N., Kempf, O., and Mulch, A., 2020, Middle Miocene long-term continental temperature change in and out of pace with marine climate records: Scientific Reports, v. 10, n. 1, p. 7989, https://doi.org/10.1038/s41598-020-64743-5

Methner, K., Mulch, A., Fiebig, J., Krsnik, E., Löffler, N., Bajnai, D., and Chamberlain, C. P., 2021, Warm High-Elevation Mid-Latitudes During the Miocene Climatic Optimum: Paleosol Clumped Isotope Temperatures From the Northern Rocky Mountains, USA: Paleoceanography and Paleoclimatology, v. 36, n. 6, https://doi.org/10.1029/2020PA003991

Mix, H. T., and Chamberlain, C. P., 2014, Stable isotope records of hydrologic change and paleotemperature from smectite in Cenozoic western North America: Geochimica et Cosmochimica Acta, v. 141, p. 532–546, https://doi.org/10.1016/j.gca.2014.07.008

Mix, H. T., Winnick, M. J., Mulch, A., and Chamberlain, C. P., 2013, Grassland expansion as an instrument of hydrologic change in Neogene western North America: Earth and Planetary Science Letters, v. 377–378, p. 73–83, https://doi.org/10.1016/j.epsl.2013.07.032

Mix, H. T., Ibarra, D. E., Mulch, A., Graham, S. A., and Chamberlain, C. P., 2016, A hot and high Eocene Sierra Nevada: Geological Society of America Bulletin, v. 128, n. 3–4, p. 531–542, https://doi.org/10.1130/B31294.1

Mix, H. T., Caves Rugenstein, J. K., Reilly, S. P., Ritch, A. J., Winnick, M. J., Kukla, T., and Chamberlain, C. P., 2019, Atmospheric flow deflection in the late Cenozoic Sierra Nevada: Earth and Planetary Science Letters, v. 518, p. 76–85, https://doi.org/10.1016/j.epsl.2019.04.050

Mulch, A., Graham, A. A., and Chamberlain, C. P., 2006, Hydrogen Isotopes in Eocene River Gravels and Paleoelevation of the Sierra Nevada: Science, v. 313, n. 5783, p. 87–89, https://doi.org/10.1126/science.1125986

Mulch, A., Teyssier, C., Cosca, M. A., and Chamberlain, C. P., 2007, Stable isotope paleoaltimetry of Eocene core complexes in the North American Cordillera: Tectonics, v. 26, n. 4, p. 1–13, https://doi.org/10.1029/2006TC001995

Mulch, A., Sarna-Wojcicki, A. M., Perkins, M. E., and Chamberlain, C. P., 2008, A Miocene to Pleistocene climate and elevation record of the Sierra Nevada (California): Proceedings of the National Academy of Sciences of the United States of America, v. 105, n. 19, p. 6819–6824, https://doi.org/10.1073/pnas.0708811105

Mulch, A., Chamberlain, C. P., Cosca, M. A., Teyssier, C., Methner, K., Hren, M. T., and Graham, S. A., 2015, Rapid change in high-elevation precipitation patterns of western North America during the Middle Eocene Climatic Optimum (MECO): American Journal of Science, v. 315, n. 4, p. 317–336, https://doi.org/10.2475/04.2015.02

Mullin, M. R. D., 2010, Stable isotope record of soil carbonates from the Eocene-Oligocene transition, Badlands National Park, South Dakota, USA: MS Thesis, Ball State University, Muncie, Indiana, http://cardinalscholar.bsu.edu/handle/123456789/194650

Nehme, C., Kluge, T., Verheyden, S., Nader, F., Charalambidou, I., Weissbach, T., Gucel, S., Cheng, H., Edwards, R. L., Satterfield, L., Eiche, E., and Claeys, P., 2020, Speleothem record from Pentadactylos cave (Cyprus): new insights into climatic variations during MIS 6 and MIS 5 in the Eastern Mediterranean: Quaternary Science Reviews, v. 250, p. 106663, https://doi.org/10.1016/j.quascirev.2020.106663

Ortiz, J. E., Torres, T., Delgado, A., Reyes, E., Llamas, J. F., Soler, V., and Raya, J., 2006, Pleistocene paleoenvironmental evolution at continental middle latitude inferred from carbon and oxygen stable isotope analysis of ostracodes from the Guadix-Baza Basin (Granada, SE Spain): Palaeogeography, Palaeoclimatology, Palaeoecology, v. 240, n. 3–4, p. 536–561, https://doi.org/10.1016/j.palaeo.2006.03.008

Page, M., Licht, A., Dupont-Nivet, G., Meijer, N., Barbolini, N., Hoorn, C., Schauer, A., Huntington, K., Bajnai, D., Fiebig, J., and Mulch, A., 2019, Synchronous cooling and decline in monsoonal rainfall in northeastern Tibet during the fall into the Oligocene icehouse: Geology, v. 47, n. 3, p. 203–206, https://doi.org/10.1130/G45480.1

Passey, B. H., and Levin, N. E., 2021, Triple Oxygen Isotopes in Meteoric Waters, Carbonates, and Biological Apatites: Implications for Continental Paleoclimate Reconstruction." Reviews in Mineralogy and Geochemistry, v. 86, n. 1, p. 429–62, https://doi.org/10.2138/rmg.2021.86.13

Passey, B. H., Ayliffe, L. K., Kaakinen, A., Zhang, Z., Eronen, J. T., Zhu, Y., Zhou, L., Cerling, T. E., and Fortelius, M., 2009, Strengthened East Asian summer monsoons during a period of high-latitude warmth? Isotopic evidence from Mio-Pliocene fossil mammals and soil carbonates from northern China: Earth and planetary science letters, v. 277, n. 3–4, p. 443–452, https://doi.org/10.1016/j.epsl.2008.11.008

Peryam, T. C., Dorsey, R. J., and Bindeman, I., 2011, Plio-Pleistocene climate change and timing of Peninsular Ranges uplift in southern California: Evidence from paleosols and stable isotopes in the Fish Creek–Vallecito basin: Palaeogeography, Palaeoclimatology, Palaeoecology, v. 305, n. 1–4, p. 65–74, https://doi.org/10.1016/j.palaeo.2011.02.014

Peters, S. E., Husson, J. M., and Czaplewski, J., 2018, Macrostrat: A platform for geological data integration and deep-time earth crust research: Geochemistry, Geophysics, Geosystems, v. 19, n. 4, p. 1393–1409, https://doi.org/10.1029/2018GC007467

Poage, M. A., and Chamberlain, C. P., 2002, Stable Isotopic Evidence for a Pre-Middle Miocene Rain Shadow in the Western Basin and Range: Implications for the Paleotopography of the Sierra Nevada: Tectonics, v. 21, n. 4, p. 16–1–16–10 https://doi.org/10.1029/2001TC001303

Poulson, S. R., and John, B. E., 2003, Stable isotope and trace element geochemistry of the basal Bouse Formation carbonate, southwestern United States: Implications for the Pliocene uplift history of the Colorado Plateau: Geological Society of America Bulletin, v. 115, n. 4, p. 434–444, https://doi.org/10.1130/0016-7606(2003)115<0434:SIATEG>2.0.CO;2

Quade, J., and Cerling, T. E., 1995, Expansion of C4 grasses in the Late Miocene of Northern Pakistan: evidence from stable isotopes in paleosols: Palaeogeography, palaeoclimatology, palaeoecology, v. 115, n. 1–4, p. 91–116, https://doi.org/10.1016/0031-0182(94)00108-K

Quade, J., Cerling, T. E., and Bowman, J. R., 1989, Development of Asian monsoon revealed by marked ecological shift during the latest Miocene in northern Pakistan: Nature, v. 342, p. 163–166, https://doi.org/10.1038/342163a0

Quade, J., Solounias, N., and Cerling, T. E., 1994, Stable isotopic evidence from paleosol carbonates and fossil teeth in Greece for forest or woodlands over the past 11 Ma: Palaeogeography, Palaeoclimatology, Palaeoecology, v. 108, n. 1–2, p. 41–53, https://doi.org/10.1016/0031-0182(94)90021-3

Quade, J., Cater, J. M., Ojha, T. P., Adam, J., and Harrison, T. M., 1995, Late Miocene environmental change in Nepal and the northern Indian subcontinent: Stable isotopic evidence from paleosols: Geological Society of America Bulletin, v. 107, n. 12, p. 1381–1397, https://doi.org/10.1130/0016-7606(1995)107<1381:LMECIN>2.3.CO;2

Retallack, G. J., Wynn, J. G., and Fremd, T. J., 2004, Glacial-interglacial–scale paleoclimatic change without large ice sheets in the Oligocene of central Oregon: Geology, v. 32, n. 4, p. 297–300, https://doi.org/10.1130/G20247.1

Ring, S. J., Bocherens, H., Wings, O., and Rabi, M., 2020, Divergent mammalian body size in a stable Eocene greenhouse climate: Scientific Reports, v. 10, n. 1, p. 3987, https://doi.org/10.1038/s41598-020-60379-7

Rothe, P., Hoefs, J., and Sonne, V., 1974, The isotopic composition of Tertiary carbonates from the Mainz Basin: an example of isotopic fractionations in "closed basins": Sedimentology, v. 21, n. 3, p. 373–395, https://doi.org/10.1111/j.1365-3091.1974.tb02066.x

Rowe, P. J., Wickens, L. B., Sahy, D., Marca, A. D., Peckover, E., Noble, S., Özkul, M., Baykara, M. O., Millar, I. L., and Andrews, J. E., 2020, Multi-proxy speleothem record of climate instability during the early last interglacial in southern Turkey: Palaeogeography, Palaeoclimatology, Palaeoecology, v. 538, p. 109422, https://doi.org/10.1016/j.palaeo.2019.109422

Rowley, D. B., and Currie, B. S., 2006, Palaeo-altimetry of the late Eocene to Miocene Lunpola basin, central Tibet: Nature, v. 439, n. 7077, p. 677–681, https://doi.org/10.1038/nature04506

Rowley, D. B., and Garzione, C. N., 2007, Stable Isotope-Based Paleoaltimetry: Annual Review of Earth and Planetary Sciences, v.35, n. 1, n. 463–508, https://doi.org/10.1146/annurev.earth.35.031306.140155

Sachse, D., Billault, I., Bowen, G. J., Chikaraishi, Y., Dawson, T. E., Feakins, S. J., Freeman, K. H., Magill, C. R., McInerney, F. A., van der Meer, M. T., Polissar, P., Robins, R. J., Sachs, J. P., Schmids, H.-L., Sessions, A. L., White, J. W. C., West, J. B., and Kahmen, A., 2012, Molecular Paleohydrology: Interpreting the Hydrogen-Isotopic Composition of Lipid Biomarkers from Photosynthesizing Organisms: Annual Review of Earth and Planetary Sciences, v. 40, n. 1, p. 221–49, https://doi.org/10.1146/annurev-earth-042711-105535

San Jose, M., Caves Rugenstein, J. K., Cosentino, D., Faccenna, C., Fellin, M. G., Ghinassi, M., and Martini, I., 2020, Stable isotope evidence for rapid uplift of the central Apennines since the late Pliocene: Earth and Planetary Science Letters, v. 544, p. 116376, https://doi.org/10.1016/j.epsl.2020.116376

Sanyal, P., Bhattacharya, S. K., Kumar, R., Ghosh, S. K., and Sangode, S. J., 2005, Palaeovegetational reconstruction in Late Miocene: A case study based on early diagenetic carbonate cement from the Indian Siwalik: Palaeogeography, Palaeoclimatology, Palaeoecology, v. 228, n. 3–4, p. 245–259, https://doi.org/10.1016/j.palaeo.2005.06.007

Saylor, J. E., Quade, J., Dettman, D. L., DeCelles, P. G., Kapp, P. A., and Ding, L., 2009, The Late Miocene Through Present Paleoelevation History of Southwestern Tibet: American Journal of Science, v. 309, n. 1, p. 1–42, https://doi.org/10.2475/01.2009.01

Scherler, L., Tütken, T., and Becker, D., 2014, Carbon and oxygen stable isotope compositions of late Pleistocene mammal teeth from dolines of Ajoie (Northwestern Switzerland): Quaternary Research, v. 82, n. 2, p. 378–387, https://doi.org/10.1016/j.yqres.2014.05.004

Schlunegger, F., Rieke-Zapp, D., and Ramseyer, K., 2007, Possible environmental effects on the evolution of the Alps-Molasse Basin system: Swiss Journal of Geosciences, v. 100, n. 3, p. 383–405, https://doi.org/10.1007/s00015-007-1238-9

Schwartz, T. M., Methner, K., Mulch, A., Graham, S. A., and Chamberlain, C. P., 2019, Paleogene topographic and climatic evolution of the Northern Rocky Mountains from integrated sedimentary and isotopic data: Geological Society of America bulletin, v. 131, n. 7–8, p. 1203–1223, https://doi.org/10.1130/B32068.1

Sharp, Z. D., 2017, Principles of Stable Isotope Geochemistry, 2nd edition, https://doi.org/10.25844/h9q1-0p82

Sjostrom, D. J., Hren, M. T., Horton, T. W., Waldbauer, J. R., and Chamberlain, C. P., 2006, Stable isotopic evidence for a pre–late Miocene elevation gradient in the Great Plains–Rocky Mountain region, USA, *in* Willett, S. D., Hovius, N., Brandon, M. T., and Fisher, D. M., editors, Tectonics, Climate, and Landscape Evolution: Geological Society of America, v. 398, p. 309–319, https://doi.org/10.1130/2006.2398(19)

Smith, G. A., Wang, Y., Cerling, T. E., and Geissman, J. W., 1993, Comparison of a paleosol-carbonate isotope record to other records of Pliocene-early Pleistocene climate in the western United States: Geology, v. 21, n. 8, p. 691–694, https://doi.org/10.1130/0091-7613(1993)021<0691:COAPCI>2.3.CO;2

Smith, M. E., Cassel, E. J., Jicha, B. R., Singer, B. S., and Canada, A. S., 2017, Hinterland drainage closure and lake formation in response to middle Eocene Farallon slab removal, Nevada, U.S.A: Earth and Planetary Science Letters, v. 479, p. 156–169, https://doi.org/10.1016/j.epsl.2017.09.023

Spencer, J.E., Harris, R.C., Dettman, D. P. J., and Patchett, 1996, Reconnaissance Survey of Upper Neogene Strata in the Bouse Formation, Hualapai Limestone, and Lower Gila River Trough, Western Arizona and Directly Adjacent Southeastern California: Arizona Geological Survey, 23 p.

Stern, L. A., Chamberlain, C. P., Reynolds, R. C., and Johnson, G. D., 1997, Oxygen isotope evidence of climate change from pedogenic clay minerals in the Himalayan molasse: Geochimica et Cosmochimica Acta, v. 61, n. 4, p. 731–744, https://doi.org/10.1016/S0016-7037(96)00367-5

Strömberg, C. A. E., 2011, Evolution of grasses and grassland ecosystems: Annual Review of Earth and Planetary Sciences, v. 39, p. 517–544, https://doi.org/10.1146/annurev-earth-040809-152402

Suarez, M. B., Passey, B. H., and Kaakinen, A., 2011, Paleosol carbonate multiple isotopologue signature of active East Asian summer monsoons during the late Miocene and Pliocene: Geology, v. 39, n. 12, p. 1151–1154, https://doi.org/10.1130/G32350.1

Sun, J., Liu, W., Liu, Z., Deng, T., Windley, B. F., and Fu, B., 2017, Extreme aridification since the beginning of the Pliocene in the Tarim Basin, western China: Palaeogeography, Palaeoclimatology, Palaeoecology, v. 485, p. 189–200, https://doi.org/10.1016/j.palaeo.2017.06.012

Super, J., ms, 2010, Hydrogen Isotope Gradients in Early Eocene British Columbia: PhD. thesis, Stanford University, Stanford, California.

Tabor, N. J., and Montañez, I. P., 2005, Oxygen and hydrogen isotope compositions of Permian pedogenic phyllosilicates: Development of modern surface domain arrays and implications for paleotemperature reconstructions: Palaeogeography, Palaeoclimatology, Palaeoecology, v. 223, n. 1–2, p. 127–146, https://doi.org/10.1016/j.palaeo.2005.04.009

Tabor, N. J., and Myers, T. S., 2015, Paleosols as Indicators of Paleoenvironment and Paleoclimate: Annual Review of Earth and Planetary Sciences, v. 43, n. 1, p. 333–61, https://doi.org/10.1146/annurev-earth-060614-105355

Tabor, N. J., Montanez, I. P., and Southard, R. J., 2002, Paleoenvironmental reconstruction from chemical and isotopic compositions of Permo-Pennsylvanian pedogenic minerals: Geochimica et Cosmochimica Acta, v. 66, n. 17, p. 3093–3107, https://doi.org/10.1016/S0016-7037(02)00879-7

Takeuchi, A., ms, 2007, Decoupling the Ancient Hydrologic System From the Modern Hydrologic System of Pacific Northwest in the United States: Implications for the Evolution of Topography, Climate, and Environment: PhD thesis, Washington State University, Pullman, Washington.

Takeuchi, A., and Larson, P. B., 2005, Oxygen isotope evidence for the late Cenozoic development of an orographic rain shadow in eastern Washington, USA: Geology, v. 33, n. 4, p.313–316, https://doi.org/10.1130/G21335.1

Takeuchi, A., Hren, M. T., Smith, S. V., Chamberlain, C. P., and Larson, P. B., 2010, Pedogenic carbonate carbon isotopic constraints on paleoprecipitation: Evolution of desert in the Pacific Northwest, USA, in response to topographic development of the Cascade Range: Chemical Geology, v. 277, n. 3–4, p. 323–335, https://doi.org/10.1016/j.chemgeo.2010.08.015

Talbot, M. R., 1990, A Review of the Palaeohydrological Interpretation of Carbon and Oxygen Isotopic Ratios in Primary Lacustrine Carbonates: Chemical Geology: Isotope Geoscience Section, v. 80, n. 4, p. 261–79, https://doi.org/10.1016/0168-9622(90)90009-2

Tang, M., Liu-Zeng, J., Hoke, G. D., Xu, Q., Wang, W., Li, Z., Zhang, J., and Wang, W., 2017, Paleoelevation reconstruction of the Paleocene-Eocene Gonjo basin, SE-central Tibet: Tectonophysics, v. 712–713, p. 170–181, https://doi.org/10.1016/j.tecto.2017.05.018

Ting, S., Bowen, G. J., Koch, P. L., Clyde, W. C., Wang, Y., Wang, Y., and McKenna, M. C., 2003, Biostratigraphic, chemostratigraphic, and magnetostratigraphic study across the Paleocene-Eocene boundary in the Hengyang Basin, Hunan, China, *in* Wing, S. L., Ginerich, P. D., Schmitz, B., and Thomas, E., editors, Causes and Consequences of Globally Warm Climates in the Early Paleogene: Geological Society of America, Special Papers, v. 369, p. 521–536, https://doi.org/10.1130/0-8137-2369-8.521

Torres, M. A., and Gaines, R. R., 2013, Paleoenvironmental and paleoclimatic interpretations of the late Paleocene goler formation, southern California, U.S.A., based on paleosol geochemistry: Journal of Sedimentary Research, v. 83, n. 8, p. 591–605, https://doi.org/10.2110/jsr.2013.48

Tütken, T., Vennemann, T. W., and Pfretzschner, H.-U., 2008, Early diagenesis of bone and tooth apatite in fluvial and marine settings: Constraints from combined oxygen isotope, nitrogen and REE analysis: Palaeogeography, Palaeoclimatology, Palaeoecology, v. 266, n. 3–4, p. 254–268, https://doi.org/10.1016/j.palaeo.2008.03.037

Vasilyan, D., and Carnevale, G., 2013, The Afro–Asian labeonine genus Garra Hamilton, 1822 (Teleostei, Cyprinidae) in the Pliocene of Central Armenia: Palaeoecological and palaeobiogeographical implications: Journal of Asian Earth Sciences, v. 62, p. 788–796, https://doi.org/10.1016/j.jseaes.2012.11.033

Vögeli, N., Najman, Y., van der Beek, P., Huyghe, P., Wynn, P. M., Govin, G., van der Veen, I., and Sachse, D., 2017, Lateral variations in vegetation in the Himalaya since the Miocene and implications for climate evolution: Earth and Planetary Science Letters, v. 471, p. 1–9, https://doi.org/10.1016/j.epsl.2017.04.037

Wang, F. B., Li, S. F., Shen, X. H., Zhang, J., and Yan, G., 1996, Formation, Evolution and Environmental Changes of the Gyirong Basin and Uplift of the Himalaya: Science in China Series D-Earth Sciences, v. 26, n. 4, p.401–409.

Wang, Y., and Deng, T., 2005, A 25 m.y. isotopic record of paleodiet and environmental change from fossil mammals and paleosols from the NE margin of the Tibetan Plateau: Earth and Planetary Science Letters, v. 236, n. 1–2, p. 322–338, https://doi.org/10.1016/j.epsl.2005.05.006

Wang, Y, Cerling, T. E., Quade, J., Bowman, J. R., Smith, G. A., and Lindsay, E. H., 1993, Stable isotopes of paleosols and fossil teeth as paleoecology and paleoclimate indicators: an example from the St. David Formation, Arizona: Washington D.C., American Geophysical Union Geophysical Monograph Series, v. 78, p. 241–248, https://doi.org/10.1029/GM078p0241

Wei, Y., Zhang, K., Garzione, C. N., Xu, Y., Song, B., and Ji, J., 2016, Low palaeoelevation of the northern Lhasa terrane during late Eocene: Fossil foraminifera and stable isotope evidence from the Gerze Basin: Scientific Reports, v. 6, n. 1, p. 27508, https://doi.org/10.1038/srep27508

White, P. D., and Schiebout, J., 2008, Paleogene paleosols and changes in pedogenesis during the initial Eocene thermal maximum: Big Bend National Park, Texas, USA: Geological Society of America Bulletin, v. 120, n. 11–12, p. 1347–1361, https://doi.org/10.1130/B25987.1

White, T., González, L., Ludvigson, G., and Poulsen, C., 2001, Middle Cretaceous greenhouse hydrologic cycle of North America: Geology, v. 29, n. 4, p. 363–366, https://doi.org/10.1130/0091-7613(2001)029<0363:MCGHCO>2.0.CO;2.

White, T., Bradley, D., Haeussler, P., and Rowley, D. B., 2017, Late Paleocene–early Eocene paleosols and a new measure of the transport distance of Alaska's Yakutat Terrane: The Journal of Geology, v. 125, n. 2, p. 113–123, https://doi.org/10.1086/690198

Williams, J. W., Grimm, E. C., Blois, J. L., Charles, D. F., Davis, E. B., Goring, S. J., Graham, R. W., Smith, A. J., Anderson, M., Arroyo-Cabrales, J., Ashworth, A. C., Betancourt, J. L., Bills, B. W., Booth, R. K., Latorre, C., Nichols, J., Purdum, T., Roth, R. E., Stryker, M., and Takahara, H., 2018, The Neotoma Paleoecology Database, a multiproxy, international, community-curated data resource: Quaternary research, v. 89, n. 1, p. 156–177, https://doi.org/10.1017/qua.2017.105

Winnick, M. J., Chamberlain, C. P., Caves, J. K., and Welker, J. M., 2014, Quantifying the isotopic 'continental effect': Earth and Planetary Science Letters, v. 406, p. 123–33, https://doi.org/10.1016/j.epsl.2014.09.005

Winnick, M. J., Welker, J. M., and Chamberlain, C. P., 2013, Stable isotopic evidence of El Niño-like atmospheric circulation in the Pliocene western United States: Climate of the Past, v. 9, n. 2, p. 903–912, https://doi.org/10.5194/cp-9-903-2013

Wolf, A., Roberts, W. H. G., Ersek, V., Johnson, K. R., and Griffiths, M. L., 2020, Rainwater isotopes in central Vietnam controlled by two oceanic moisture sources and rainout effects: Scientific reports, v. 10, p. 16482, https://doi.org/10.1038/s41598-020-73508-z

Xia, Z., and Winnick, M. J., 2021, The competing effects of terrestrial evapotranspiration and raindrop re-evaporation on the deuterium excess of continental precipitation: Earth and Planetary Science Letters, v. 572, p. 117120, https://doi.org/10.1016/j.epsl.2021.117120

Xu, Q., Ding, L., Zhang, L., Cai, F., Lai, Q., Yang, D., and Liu-Zeng, J., 2013, Paleogene high elevations in the Qiangtang Terrane, central Tibetan Plateau: Earth and Planetary Science Letters, v. 362, p. 31–42, https://doi.org/10.1016/j.epsl.2012.11.058

Xu, Q., Ding, L., Hetzel, R., Yue, Y., and Rades, E. F., 2015, Low elevation of the northern Lhasa terrane in the Eocene: Implications for relief development in south Tibet: Terra Nova, v. 27, n. 6, p. 458–466, https://doi.org/10.1111/ter.12180

Xu, Q., Liu, X., and Ding, L., 2016, Miocene high-elevation landscape of the eastern Tibetan Plateau: Geochemistry, Geophysics, Geosystems, v. 17, n. 10, p. 4254–4267, https://doi.org/10.1002/2016GC006437

Zamanian, K., Pustovoytov, K., and Kuzyakov, Y., 2016, Pedogenic Carbonates: Forms and Formation Processes: Earth-Science Reviews, v. 157, p. 1–17, https://doi.org/10.1016/j.earscirev.2016.03.003

Zamarreno, I., Anadon, P., and Utrilla, R., 1997, Sedimentology and isotopic composition of Upper Palaeocene to Eocene non-marine stromatolites, eastern Ebro Basin, NE Spain: Sedimentology, v. 44, n. 1, p. 159–176, https://doi.org/10.1111/j.1365-3091.1997.tb00430.x

Zanazzi, A., Kohn, M. J., MacFadden, B. J., and Terry, D. O., 2007, Large temperature drop across the Eocene-Oligocene transition in central North America: Nature, v. 445, p. 639–642, https://doi.org/10.1038/nature05551

Zanazzi, A., Judd, E., Fletcher, A., Bryant, H., and Kohn, M. J., 2015, Eocene–Oligocene latitudinal climate gradients in North America inferred from stable isotope ratios in perissodactyl tooth enamel: Palaeogeography, Palaeoclimatology, Palaeoecology, v. 417, p. 561–568, https://doi.org/10.1016/j.palaeo.2014.10.024

Zhisheng, A., Yongsong, H., Weiguo, L., Zhengtang, G., Clemens, S., Li, L., Prell, W., Youfeng, N., Yanjun, C., Weijian, Z., Benhai, L., Qingle, Z., Yunning, C., Xiaoke, Q., Hong, C., and Zhenkun, W., 2005, Multiple Expansions of C4 Plant Biomass in East Asia Since 7 Ma Coupled with Strengthened Monsoon Circulation: Geology, v. 33, n. 9, p. 705–708, https://doi.org/10.1130/G21423.1

Zhuang, G., Hourigan, J. K., Koch, P. L., Ritts, B. D., and Kent-Corson, M. L., 2011, Isotopic constraints on intensified aridity in Central Asia around 12Ma: Earth and Planetary Science Letters, v. 312, n. 1–2, p. 152–163, https://doi.org/10.1016/j.epsl.2011.10.005